

10-14-1980

An Analysis of Gravity Surveys in the Portland Basin, Oregon

Janice C. Perttu
Portland State University

Follow this and additional works at: https://pdxscholar.library.pdx.edu/open_access_etds



Part of the [Geology Commons](#), and the [Geophysics and Seismology Commons](#)

Let us know how access to this document benefits you.

Recommended Citation

Perttu, Janice C., "An Analysis of Gravity Surveys in the Portland Basin, Oregon" (1980). *Dissertations and Theses*. Paper 3199.

<https://doi.org/10.15760/etd.3190>

This Thesis is brought to you for free and open access. It has been accepted for inclusion in Dissertations and Theses by an authorized administrator of PDXScholar. Please contact us if we can make this document more accessible: pdxscholar@pdx.edu.

AN ABSTRACT OF THE THESIS OF Janice C. Perttu for the
Master of Science in Geology presented October 14, 1980.

Title: An Analysis of Gravity Surveys in the Portland
Basin, Oregon.

APPROVED BY MEMBERS OF THE THESIS COMMITTEE:


Ansel G. Johnson, Chairman


Gilbert T. Benson


Marvin H. Beeson


Michael L. Cummings

The geologic setting of the Portland Basin is ideal for gravity surveys because of the large density contrasts between geologic units. The Portland Basin consists of a north-northwest-trending syncline in the Columbia River basalt overlain by Pliocene to Recent alluvium. This study was undertaken to define structures in the Portland Basin which are obscured by the alluvium.

An areal gravity survey of the Portland Basin covering approximately 450 square kilometers was conducted for this study. Gravity values at approximately 350

locations in the study area were measured by the author and an additional 400 previously measured stations were included in the analysis. The data were reduced by computer methods to complete Bouguer gravity values which were contoured at a one milligal interval. The resulting Complete Bouguer Gravity Anomaly Map of the Portland Basin is generally consistent with the Complete Bouguer Gravity Anomaly Map of Oregon by Berg and Thiruvathukal (1967). The primary features shown on the map are a gravity high, which extends throughout the western half of the study area, and decreasing gravity values in the eastern half of the study area, reflecting the thickening crust at depth. In the southwest corner of the study area, the gravity high branches into north-trending and northwest-trending noses, which are separated by a northwest-trending linear feature which coincides with the Portland Hills Fault trend.

Four east-west-trending lines were modeled by computer methods. All models show a broad bottomed syncline beneath the Portland Basin with or without graben-like faulting. With the exception of the Portland Hills Fault trend, the faults do not appear to define any continuous trends. One model shows a vertical offset along the Portland Hills Fault of 120 meters. No structural features in the Columbia River basalt coinciding with the Boring Lava vent locations were delineated.

An abrupt lateral contact between Eocene through Oligocene sedimentary rocks and contemporaneous volcanic rocks is indicated by deep wells in the Portland area. This contact, referred to as the "sediment-volcanic interface" in this study, is reflected in the gravity values and is located on each model. These locations form a north-northwest trend south of the northernmost model, the Columbia Boulevard model. The interface is located east of this trend on the Columbia Boulevard model, and this displacement may represent 20 to 50 km of right-lateral movement on the Portland Hills Fault if it was part of a continuous structure with the other locations.

The gravity high in the western half of the study area was modeled with an intrusion, having a density of 3.0 gm/cm^3 . The modeled intrusion is sill-shaped and increases in thickness to the south. It is spatially related to both the Skamania Volcanics and the Boring Lavas and consequently could be genetically related to either volcanic episode.

AN ANALYSIS OF GRAVITY SURVEYS IN THE
PORTLAND BASIN, OREGON

by
JANICE C. PERTTU

A thesis submitted in partial fulfillment of the
requirements for the degree of

MASTER OF SCIENCE
in
GEOLOGY

Portland State University

1981

TO THE OFFICE OF GRADUATE STUDIES AND RESEARCH:

The members of the Committee approve the thesis of
Janice C. Perttu presented October 14, 1980.

[REDACTED]
Ansel G. Johnson, Chairman

[REDACTED]
Gilbert T. Benson

[REDACTED]
Marvin H. Beeson

[REDACTED]
Michael L. Cummings

APPROVED:

[REDACTED]
Ansel G. Johnson, Head, Department of Earth Science

[REDACTED]
Stanley Rauch, Dean of Graduate Studies and Research

ACKNOWLEDGEMENTS

I would like to thank my advisor, Dr. Ansel G. Johnson, for his assistance throughout the duration of this study. I am also grateful to the members of my thesis committee, my husband, Rauno, and all others who critically reviewed this text, and to Drs. R. Couch and Z.F. Danes for the loan of their gravimeters.

TABLE OF CONTENTS

	PAGE
ACKNOWLEDGEMENTS	iii
LIST OF TABLES	vi
LIST OF FIGURES	vii
LIST OF PLATES	ix
INTRODUCTION	1
Purpose of Study	1
Location and Extent of Gravity Surveys	1
Previous Work	2
GEOLOGY	5
Stratigraphy	5
Structure and Tectonics	14
GRAVITY	19
Introduction	19
Objectives	19
Gravity Survey	25
Data Reduction	27
Data Compilation	28
Modeling	33
Previous Models	57
Areal Compilation of Gravity Models	61

	PAGE
Geologic Implications of the Gravity Models . .	69
Regional Implications	83
CONCLUSIONS	84
REFERENCES CITED	87
APPENDIX	93

LIST OF TABLES

TABLE		PAGE
I	Stratigraphic Units Used in Models	34
II	Gravity Data	93

LIST OF FIGURES

FIGURE	PAGE
1. Location map	3
2. Geologic map of Portland and vicinity, from Wells and Peck (1961) and Huntting and others (1961)	6
3. Tualatin Basin-Portland Basin subsurface cross-section, from Newton (1969)	7
4. Preliminary tectonic map of the greater Portland area, from Benson and Donovan (1974).	22
5. Complete Bouguer gravity anomaly map of Portland and vicinity, from Berg and Thiruvathukal (1967) and Bonini, Hughes, and Danes (1974)	24
6. Comparison of the Complete Bouguer Gravity Anomaly Map of Oregon (Berg and Thiru- vathukal, 1967) and the Complete Bouguer Gravity Anomaly Map of the Portland Basin	31
7. Columbia Boulevard 1 gravity model	37
8. Columbia Boulevard 2 gravity model	38
9. Stark Street 1 gravity model	42

FIGURE	PAGE
10. Stark Street 2 gravity model	43
11. Stark Street 3 gravity model	44
12. Holgate Boulevard 1 gravity model	50
13. Holgate Boulevard 2 gravity model	51
14. Clackamas Highway gravity model	54
15. Kings Heights-Albina Line gravity model	59
16. Sellwood Line gravity model	60
17. Oak Grove Line gravity model	62
18. Gravity model compilation	64
19. Mt. Scott topography and density profile. Densities in gm/cm ³	70
20. Spatial relationship between the modeled intrusion and Boring Lava occurrences	75
21. Schematic illustration of right-lateral off- set on the Portland Hills Fault	79

LIST OF PLATES

PLATE	PAGE
1. Complete Bouguer Gravity Anomaly Map of the Portland Basin	pocket
2. Residual Complete Bouguer Gravity Anomaly Map of the Portland Basin	pocket

INTRODUCTION

PURPOSE OF STUDY

The Portland Basin is a structural basin formed by downwarping of the Columbia River basalt. Pliocene to Recent alluvial materials filled the basin, obscuring the bedrock and any structures within the Columbia River basalt. Consequently many prior investigations in the Portland Basin concentrated on topics having more accessible geologic data, while giving only a cursory examination to the structural geology. Lack of outcrops, dense urbanization, and large density contrast between the Columbia River basalt and overlying alluvium make gravity surveys the most economical and practical method for increasing our knowledge of the structural geology in the Portland Basin.

LOCATION AND EXTENT OF GRAVITY SURVEYS

The study area is located at the northern end of the Willamette Valley in northwest Oregon. It includes the municipalities of Fairview, Wood Village, Troutdale, Gresham, Boring, Damascus, Clackamas, Gladstone, and Milwaukie, as well as the eastern portion of Portland. The study area covers about 450 square kilometers and

is bounded on the west by the Willamette River, on the north by the Columbia River, on the east by the Sandy River and the eastern boundary of R. 3 E., W.M., and on the south by the Clackamas River as shown in Figure 1. The Tualatin Mountains (Portland Hills) trend northwest and lie west of the Willamette River, separating the Tualatin Valley and the Portland Basin. The foothills of the Cascades rise gently to the east of the study area.

Some gravity stations located west of the Willamette River and south of the Clackamas River are included for completeness.

Nearly all of the area is developed into business or residential areas.

PREVIOUS WORK

The geology of the Portland area was described by Treasher (1942) and Trimble (1963). Hammond and others (1974) investigated surficial features and the seismic history of the Portland area. In 1976, Beeson and others studied the stratigraphy, structure, and distribution of the Columbia River basalt in the Portland area with emphasis on the Portland Hills west of the study area, and Burch (in progress) analyzed the trace element geochemistry of the Boring Lavas in the Portland metropolitan area.

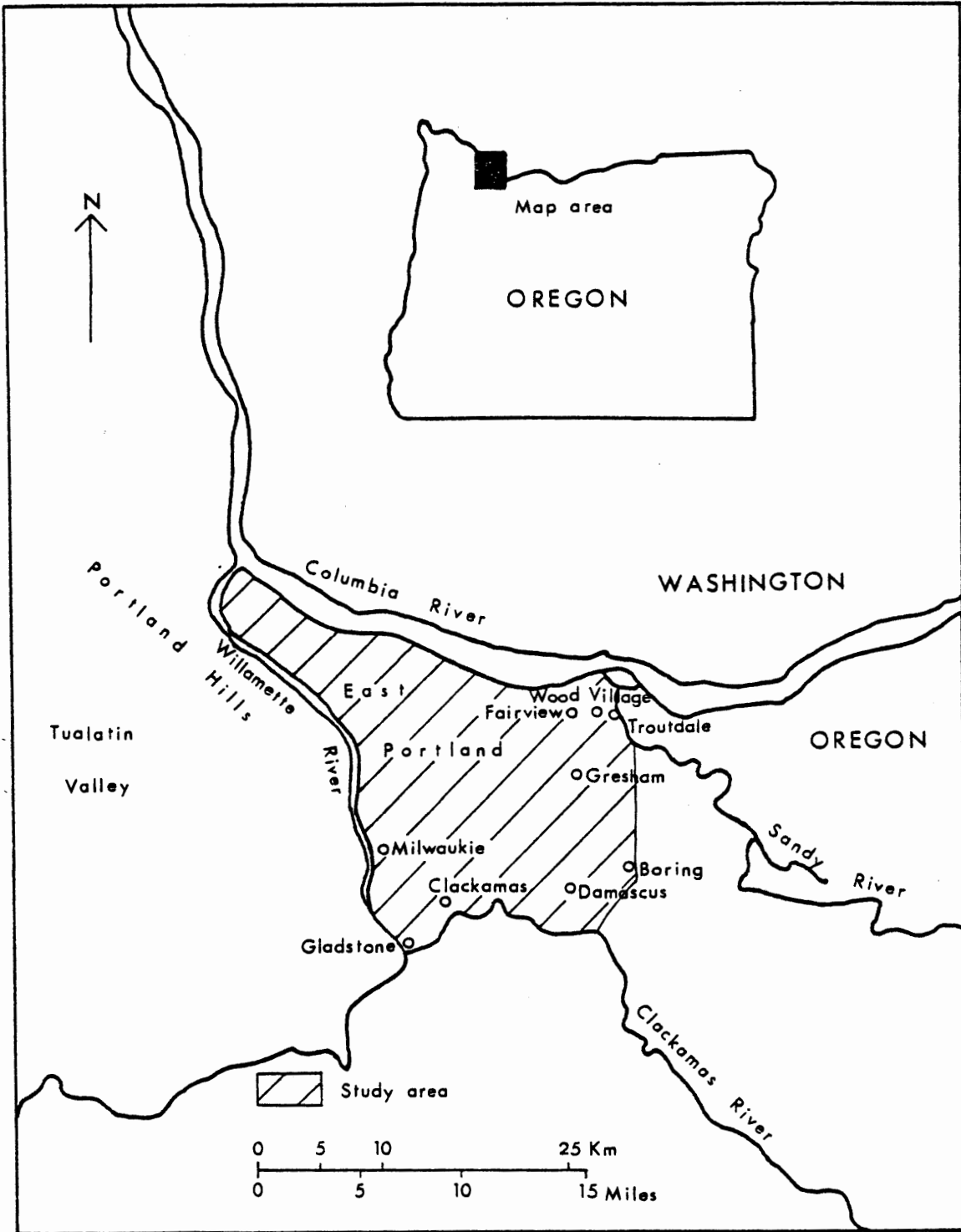


Figure 1. Location map.

General geologic investigations of broader scope, but including the study area include Diller (1896), Snavely and Wagner (1963), and Newton (1969). Ground water reports by Piper (1942), Griffin, Watkins and Swenson (1956), and Hogenson and Foxworthy (1965) include the study area.

The "Complete Bouguer Gravity Anomaly Map of Oregon" prepared by Berg and Thiruvathukal (1967), the analysis of these data in Thiruvathukal and others (1970), and the "Complete Bouguer Gravity Anomaly Map of Washington" by Bonini, Hughes, and Danes (1974) provided a regional framework of gravity data for this study. A regional gravity and aeromagnetic analysis by Bromery and Snavely (1964) covers northwestern Oregon west of the study area. Previous local gravity surveys incorporated in this study were conducted by Schmela (1971), Cash (unpublished, 1973), Johnson and others (1976), and Jones (1977). Gravity trends from data collected by the author in 1974 are shown on the "Preliminary Tectonic Map of the Greater Portland Area" (Benson and Donovan, 1974).

GEOLOGY

STRATIGRAPHY

Introduction

Figure 2 is a generalized geologic map of the study area and adjacent areas. The oldest unit exposed in the study area is the Columbia River Basalt Group of middle to late Miocene age. Pliocene to Recent sedimentary units overlying the Columbia River basalt are not differentiated. Realistic gravity modeling requires the inclusion of units which occur at depth and in adjacent areas. Two deep wells west of the study area, the Richfield Oil Barber well (Barber well) and the Texaco Inc. Cooper Mountain well (Cooper Mountain well), provide valuable information on the underlying formations, and outcrops in the Portland Hills show structures adjacent to the study area. Figure 3 is a geologic cross-section through the study area from Newton (1969) based on information from these wells and shallower wells in the study area. In the remainder of the text, the vertical locations of all stratigraphic horizons are described as elevations above or below mean sea level rather than as depths below the ground surface.

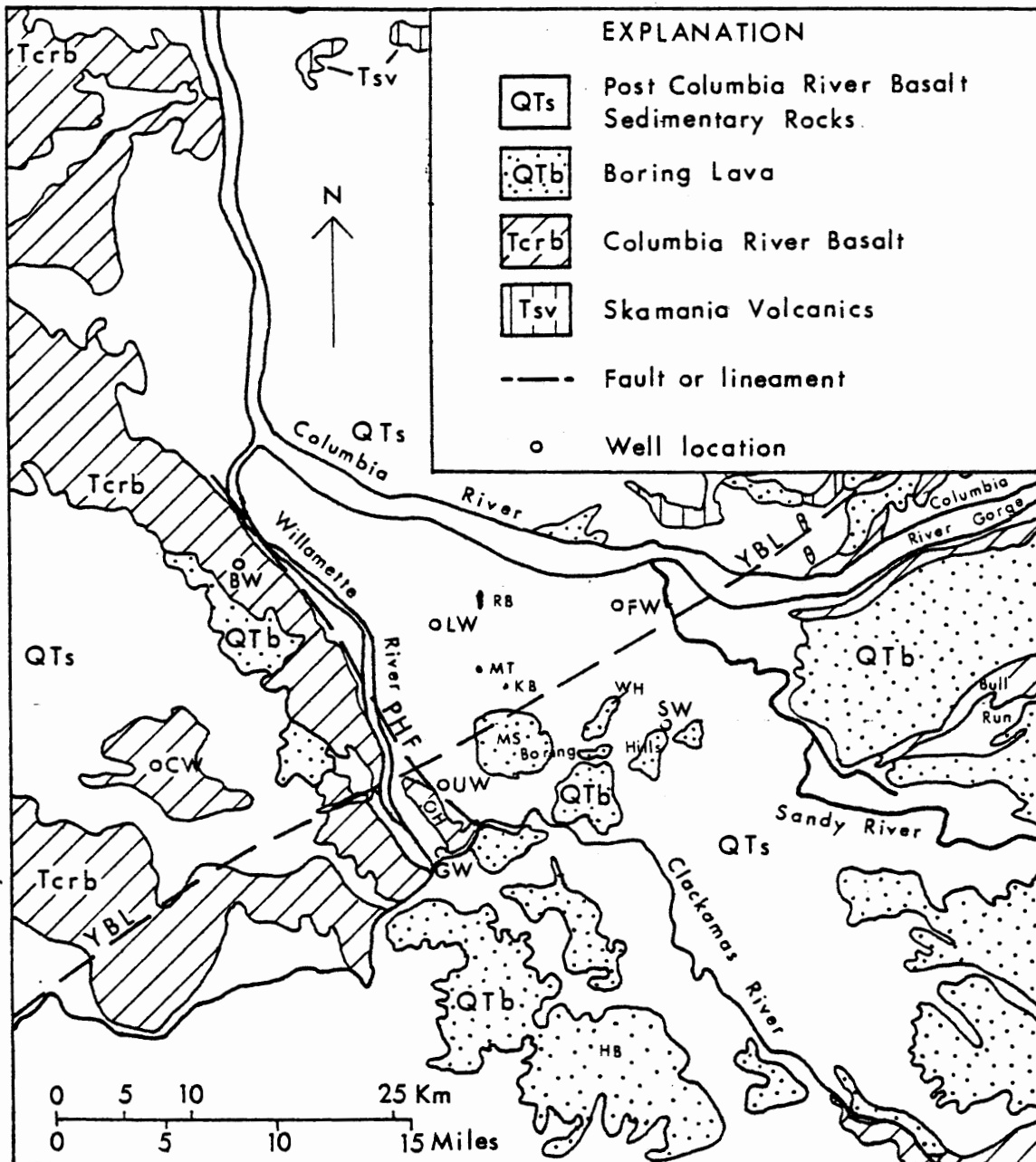


Figure 2. Geologic map of Portland and vicinity, from Wells and Peck (1961) and Hunting and others (1961). Abbreviations: BW = Barber well; CW = Cooper Mountain well; FW = Fairview well; GW = Gladstone well; HB = Highland Butte; KB = Kelly Butte; LW = Ladd well; MS = Mt. Scott; MT = Mt. Tabor; OH = Oatfield Hill; PHF = Portland Hills Fault; RB = Rocky Butte; SW = Shiiki well; UW = Union H.S. well; WH = Walters Hill; YBL = Yamhill-Bonneville Lineament.

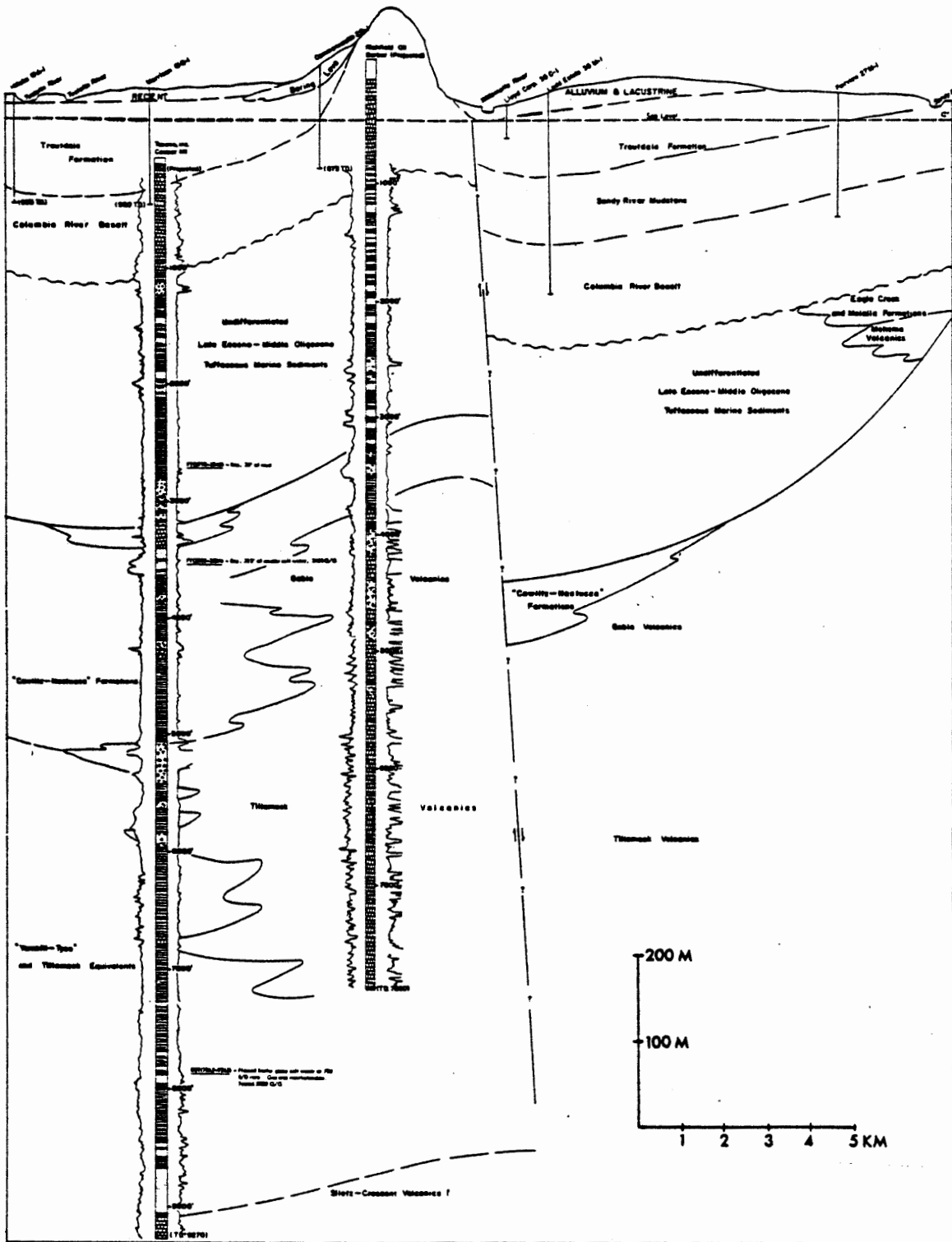


Figure 3. Tualatin Basin-Portland Basin subsurface cross-section, from Newton (1969)

Siletz River Volcanic Series

The Siletz River Volcanic Series is the oldest unit exposed in northwest Oregon and encountered in wells in the Portland area. Originally described by Snavely and Baldwin (1948), this series consists of early to middle Eocene pillow lava and basaltic fragmental debris with intercalated volcanoclastic and marine sedimentary rocks (Snavely and Wagner, 1964) which crop out in the central Coast Range and along the western margin of the Willamette Valley (Beaulieu, 1971). Snavely and others (1968) analyzed the chemistry of the Siletz River Volcanic Series and divided it into a lower, more primitive unit of ocean ridge tholeiites, overlain by an upper unit, consisting of predominantly alkalic tholeiites following a Hawaiian trend of chemical variation. Units described and referred to as the Tillamook Volcanic Series by Warren, Norbistrath, and Grivetti (1945) are included in the Siletz River Volcanic Series in this study.

The Cooper Mountain well intercepts the top of the Siletz River Volcanic Series at about -2800 meters (m) (-9200 feet (ft)) as shown in Figure 3. The location of the unit in the Barber well is not well defined, because it is overlain in this area by Skamania Volcanics which are difficult to distinguish from the Siletz River Volcanics on the basis of the well log data.

Eocene Sedimentary Rocks

The Yamhill-Tyee equivalents and the Cowlitz-Nestucca Formation shown on Figure 3 are combined in the gravity modeling because of their similar densities and are referred to as "Eocene Sedimentary Rocks". Marine siltstones and shales with minor sandstones and basalt flows of probable middle Eocene age unconformably overlie the Siletz River Volcanic Series (Snively and Wagner, 1963; Newton, 1969). These sediments may be equivalent to the Yamhill Formation described by Baldwin and others (1955), or to the Tyee Formation described by Diller (1898), Newton (1969), and Snively and Wagner (1963). These rocks are at least 1000 m (3300 ft) thick in the Cooper Mountain well, but are absent in the Barber well, as shown in Figure 3, indicating rapid thinning to the east.

Thin-bedded tuffaceous siltstones and massive sandstones, referred to locally as the Cowlitz-Nestucca Formation, overlie the Yamhill-Tyee equivalents (Newton, 1969). This designation is applied to these units because of lithologic and stratigraphic similarities to the Cowlitz and Nestucca Formations which are exposed north and west of the study area (Weaver, 1912; Snively and Vokes, 1949; Newton, 1969). The Cowlitz-Nestucca section in the Cooper Mountain well shows a large proportion of volcanic breccias and agglomerates, probably because of the close proximity of centers of

contemporaneous volcanism to the east.

The Cowlitz-Nestucca rocks occur in both deep wells, but thin rapidly eastward from about 660 m (2160 ft) in the Cooper Mountain well to about 170 m (550 ft) in the Barber well.

Skamania Volcanic Series

Altered basalt, basaltic andesite, and pyroclastic rocks of the Skamania Volcanic Series (Felts, 1939a and 1939b) are exposed both north and south of the study area (Trimble, 1963). The area of outcrop south of the study area is located along the Willamette River south of the Gladstone well (GW), but is too small to appear on Figure 2. Trimble (1963) suggested a late Eocene to early Miocene age for this series and divides it into a lower, altered and deformed unit and an upper, unaltered and undeformed unit. The Goble Volcanics (Warren, Norbistrath, and Grivetti, 1945), consisting of porphyritic basalt flows, breccias, and pyroclastic rocks, outcrop northwest of the study area along the Columbia River and interfinger with the Cowlitz-Nestucca Formation (Snively and Wagner, 1964). Trimble (1963) suggested that the Goble Volcanics may be correlative with the lower unit of the Skamania Volcanics. Beck and Burr (1979) included rocks north of the Columbia River which were mapped as Skamania Volcanic Series by Trimble (1963) in the Goble

Volcanic Series; and Newton (1969) refers to the volcanic sequence intercepted in the Barber well as Goble Volcanics. On the other hand, Hammond (personal communication, 1980) believes that the Skamania Volcanic Series may be more closely related to the middle and upper portions of the Ohanapecosh Formation which occurs east of the study area. In this study, any late Eocene to early Miocene volcanic rocks will be referred to as part of the Skamania Volcanic Series.

Late Eocene to Oligocene Sedimentary Rocks

During latest Eocene and Oligocene time, tuffaceous marine shales, sandstones, and conglomerates were deposited in the Portland area (Trimble, 1963; Snavely and Wagner, 1963; Newton, 1969). The Skamania Volcanic Series may have been the source of the tuffaceous material (Trimble, 1963). These rocks may be equivalent to the Spencer Formation (Turner, 1938), the Pittsburg Bluff Formation (Schenck, 1927), and the Scappoose Formation (Warren and Norbistrath, 1946), all of which crop out along the western margin of the Tualatin Valley, but have not been differentiated on the basis of the well log data. The well log data indicate that these deposits occur farther east in the Portland area than the Cowlitz-Nestucca deposits (Figure 3) and Snavely and Wagner (1963) place the eastern boundary of marine deposition during Oligocene time at approximately the foothills of the

Cascades. These sedimentary rocks are intercepted in both the Cooper Mountain and Barber wells and maintain a thickness of about 600 m (2000 ft) in each. Also interpreted as part of this unit are 40 m (125 ft) of material listed as blue clay, tuffaceous sandstone and broken rock in the Fairview well.

Columbia River Basalt Group

The late Eocene to Oligocene sedimentary rocks are unconformably overlain by flows of the Columbia River Basalt Group. The Columbia River basalt is the oldest unit exposed in the study area. It crops out only in the extreme southwest corner of the study area, but is widely exposed in the Portland Hills immediately to the west of the study area. East of the area, a small exposure occurs along the Sandy River, with extensive exposures farther east in the Columbia River Gorge and in the Bull Run watershed.

The Columbia River basalt (Russel, 1893) is dark-gray, dense, and finely crystalline, showing predominantly columnar and blocky jointing. Of the over 20 flows identified in the Portland area by Beeson and others (1976), 18 are correlated with flows of the Yakima Basalt Subgroup in eastern Oregon and Washington (Beeson, Bentley, and Moran, 1976). Flow groups identified in the Portland area which also occur in the Columbia

Plateau are the Grande Ronde Basalt and the Wanapun Basalt. The total thickness of the Columbia River basalt in the Portland area varies from about 330 m (1000 ft) in the Cooper Mountain well to about 180 m (580 ft) in the Fairview and Gladstone wells (Figures 2 and 3).

Post Columbia River Basalt Sedimentary Rocks

Warping of the Columbia River basalt formed basins which are filled with Pliocene fluvial and lacustrine sediments. In the study area, the Columbia River basalt is overlain by the Sandy River mudstone, which is exposed in the Sandy River and the Clackamas River and their tributaries (Trimble, 1963). This unit consists predominantly of beds of siltstone or fine sandstone. Overlying the Sandy River mudstone is a sequence of well indurated fluvial sandstones and conglomerates known as the Troutdale Formation (Hodge, 1933). The Troutdale Formation is also exposed in the Sandy and Clackamas River valleys and crops out on many topographic highs (Trimble, 1963) such as Mt. Scott and Mt. Tabor, located on Figure 2.

During Pleistocene time, mudflows and gravels filled in existing topographic lows and later lacustrine deposits blanketed most of the Portland Basin (Trimble, 1963). Recent alluvium covers the flood plains of the Columbia and Willamette Rivers and their tributaries up to an elevation

of about 15 m (50 ft). All post-Columbia River basalt sedimentary rocks are grouped as a single unit for gravity modeling purposes. R.O. Van Atta (personal communication to A. Johnson, 1975) indicated that the equivalent sediments in the Tualatin Valley have a lower density than those in the Portland Basin.

Boring Lava

After extensive erosion of the Troutdale Formation, basaltic flows and minor amounts of pyroclastics, known as the Boring Lava (Treasher, 1942), were erupted from vents in the Portland area, forming conical hills (the Boring Hills, shown on Figure 2) or broad lava plains such as the occurrences shown south of the Clackamas River and east of the Sandy River on Figure 2 (Trimble, 1963). The Boring Lava is a light-gray, pilotaxitic to diktytactic, olivine basalt which is commonly weathered to a depth of 8 m (25 ft) or more (Trimble, 1963). In the study area, these volcanics occur primarily in the Boring Hills, but also occur at Mt. Tabor, Rocky Butte, and Kelly Butte.

STRUCTURE AND TECTONICS

The following section presents a simplified overview of the tectonic history of northwest Oregon. This summary will not elaborate on current matters of debate, but rather will attempt to construct a regional framework

within which the structure and tectonics in the Portland area can be discussed.

The oldest rocks in northwest Oregon, the Siletz River Volcanic Series, are interpreted as ocean ridge tholeiites overlain by seamounts on the basis of geochemical data (Snively and others, 1968). In early Eocene time, a subduction zone existed just west of the present Cascade Range trend (Atwater, 1970; Maxwell, 1974). The Siletz River Volcanic Series was probably part of the oceanic plate moving towards this subduction zone.

In middle Eocene time, the subduction zone moved abruptly westward possibly because of jamming of the subduction zone by seamounts (Perttu, 1976) or by an aseismic ridge (Simpson and Cox, 1977), or because of changes in plate motions. A fore-arc basin formed near the present Puget-Willamette Lowland behind the newly formed coastal mountains. The Tyee and Fluornoy Formations were deposited in this basin south of the study area. The typically thick-bedded Tyee Formation and rhythmically bedded Fluornoy Formation (Baldwin, 1975) have been interpreted as representing continental shelf and slope deposits respectively (Perttu and Benson, 1980). The coeval Yamhill-Tyee section in the Portland area is much thinner than the Tyee Formation to the south, probably as a consequence of having been deposited in an area having less rapid sedimentation.

During late Eocene time, localized uplift and volcanism divided the fore-arc basin into several basins (Snively and Wagner, 1963). Marine sedimentation continued west of about 123 degrees longitude while basaltic and andesitic volcanism occurred east of this boundary (Snively and Wagner, 1963). The Cowlitz-Nestucca Formation interfingers with the Skamania Volcanic Series and Goble Volcanics along this boundary as shown in Figure 3. This figure suggests that this sediment-volcanic boundary existing during deposition of the earlier Tye-Yamhill equivalents as well. Beck and Burr (1979) suggest that the Skamania Volcanics may represent the initial stages of the formation of a volcanic arc.

Recent magnetic studies by Simpson and Cox (1977) indicate that the Tye Formation and the Siletz River Volcanic Series are rotated 50 to 70 degrees clockwise from the Eocene magnetic field direction. They postulate that rotation began during late Eocene time, possibly as the result of back-arc spreading or changes in plate motion.

Late Eocene and Oligocene time seem to have been a period of lessened tectonic activity in northwest Oregon. Lignitic siltstones and glauconite zones occur in sediments deposited at this time and the upper unit of the Skamania Volcanic Series is undeformed and unaltered.

Rotation apparently continued at least through Oligocene time (Simpson and Cox, 1977; Beck and Burr, 1979).

During Miocene time, marine deposition shifted westward to approximately the present day shoreline, and erosion and deformation produced an uneven surface in the Portland area onto which middle to late Miocene flood basalts flowed (Trimble, 1963). Detailed stratigraphic studies of the Columbia River Basalt Group in the Portland area by Beeson and others (1976) show that deformation continued as successive flows entered the Portland area. The development of the Portland Hills anticline apparently prevented all post-Grande Ronde Basalts from crossing its axis to the west. The Tualatin and Portland Basins formed as gentle synclines adjacent to both sides of the Portland Hills.

Geomorphic and structural evidence discussed by Balsillie and Benson (1971) suggests that the northeast side of the Portland Hills may be fault bounded. The structure, shown in Figure 3 as a normal fault, down to the east, has been informally named the Portland Hills Fault. The interpretation of gravity lines run across the structure by Johnson and others (1976) and Jones (1977) are consistent with vertical offsets of about 200 meters and 300 meters respectively. Modeling by Johnson and others (1976) also suggests the presence of other faults

east of the Portland Hills Fault. Evidence supporting a predominantly right-lateral sense of movement along the Portland Hills Fault since Eocene time is described in Beeson and others (1976) and Jones (1977). Beeson and others (1976) proposed that the Portland Hills formed as a result of slow and continuous right-lateral movement along the Portland Hills Fault. They attribute the sense of movement on the fault to a variant of Basin and Range extension which may be pushing the southwest block north and west past the northeast block. Anderson (1978) has also found evidence in the Columbia River basalt in the Clackamas River drainage suggesting right-lateral movement. Units overlying the Troutdale Formation show little evidence of deformation (Trimble, 1963).

GRAVITY

INTRODUCTION

Local gravity anomalies are the result of horizontal variations in earth material density. To produce an anomaly from originally flat-lying strata, there must be a density contrast between the layers and the layers must be deformed in some way. The magnitude and shape of the anomaly will depend on the densities of the materials and the depth and geometry of their occurrence (Nettleton, 1971).

OBJECTIVES

Trimble (1963) described the structural geology of the Portland area as simple; consisting of broad synclinal folds separated by an equally broad anticline with minor faulting. Detailed studies in recent years (Beeson and others, 1976; Johnson, 1975; Jones, 1977) aided by geochemical and geophysical techniques in addition to field mapping, have shown considerable complexity in areas where sufficient data have been gathered. The extensive alluvial cover in the Portland Basin has prevented the analysis of the bedrock geology by normal field mapping techniques, and the extensive urbanization prohibits the use of ground magnetic and seismic methods. Gravity

surveys on the other hand, can provide valuable information in such situations. Using gravity data, this study investigates structures in the Columbia River basalt, the interface between Eocene to Oligocene sedimentary and volcanic rocks, a postulated high density intrusion, and Boring Lava occurrences.

Structures in the Columbia River Basalt

Identification of faults within the Columbia River basalt in the Portland Basin is one of the primary objectives of this study. The large density contrast between the basalt and the overlying sedimentary rocks facilitates this process. As shown on Figure 2, most of the Portland Hills Fault lies west of the study area, and consequently it was not a prime focus of this study. The fault does pass through the southwest corner of the study area where detailed data were gathered across the fault trace.

The interpretation of gravity surveys conducted by Johnson and others (1976) shows faults having offsets on the order of 150 meters east of the Portland Hills Fault beneath the Portland Basin. The orientation of these faults was assumed to be parallel to the Portland Hills Fault trend (N40W). This study attempts to identify other such offsets in the Columbia River basalt and determine if any continuous structural trends can be identified.

Hammond (1971) suggested the possible existence of a northeast-trending left-lateral transform fault zone referred to as the Yamhill-Bonneville Lineament through the Portland Basin. His location of this structure is shown on Figure 2. The gravity data will be examined to see if any structural expression of this zone is reflected in the data.

The term "Portland Basin" is an informal name given to the syncline underlying East Portland. Figure 4 is a portion of the "Preliminary Tectonic Map of the Greater Portland Area" by Benson and Donovan (1974) which shows the configuration of the basin reflected by the structure of the Columbia River basalt determined from well log data. The gravity data should reflect any major deviations from this interpretation.

Eocene to Oligocene Sediment-Volcanic Interface

Rocks of the Skamania Volcanic Series crop out north and south of the study area suggesting they underlie the area as well. Figure 3 shows this interpretation and the sharp lateral boundary between the volcanic rocks and the contemporaneous sedimentary rocks. The large density contrast between the sediments and the volcanics should allow the accurate location of this interface. In subsequent discussions, this feature will be referred to as the "sediment-volcanic interface". Modeling by Johnson and others (1976) and Jones (1977) indicates that this

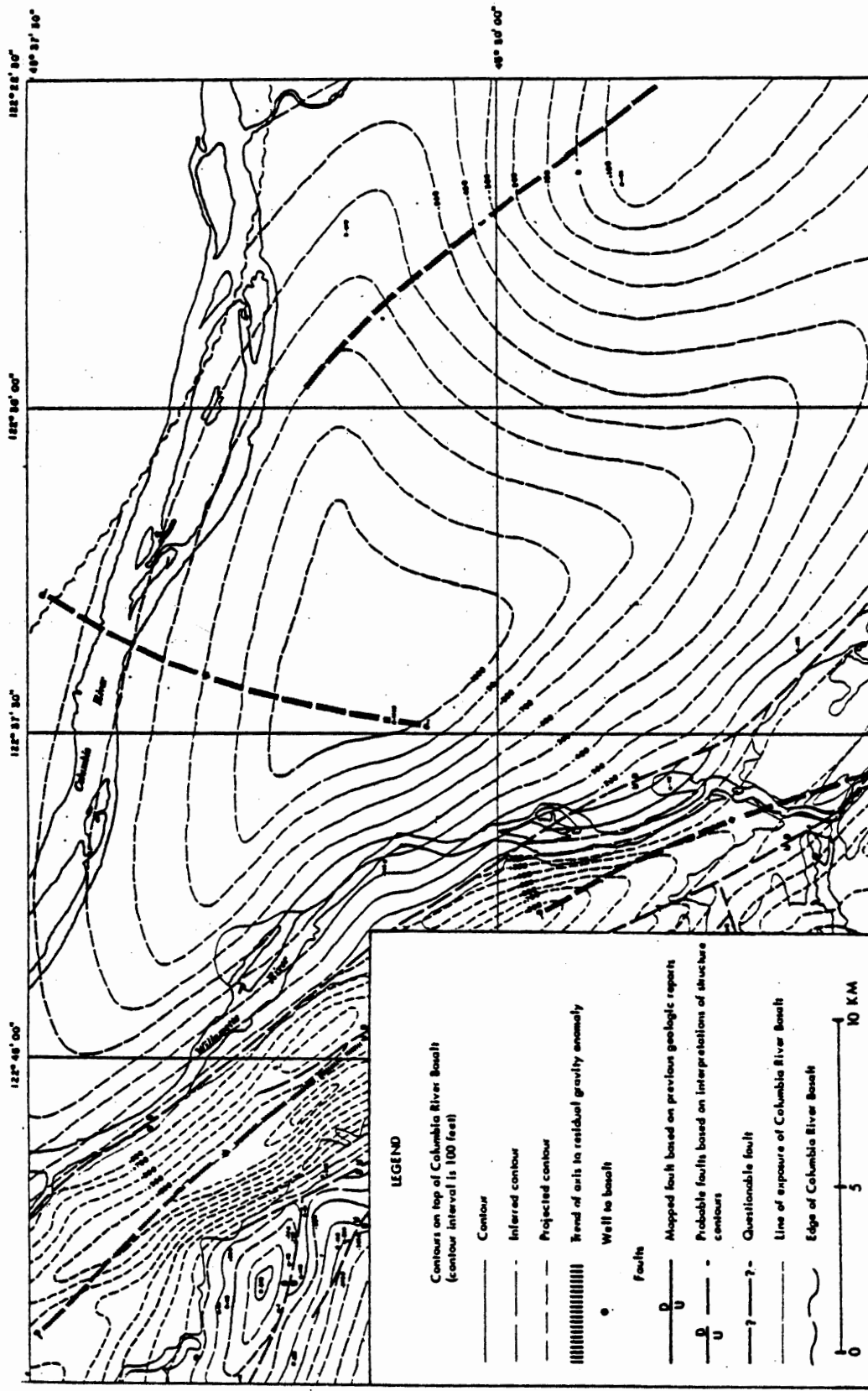


Figure 4. Preliminary tectonic map of the greater Portland area, from Benson and Donovan (1974).

interface runs roughly north-south beneath the Portland Hills. Data from this study will provide further information on the trend of this feature.

Intrusion

The Complete Bouguer Gravity Anomaly Map of Oregon (Berg and Thiruvathukal, 1967) and the Complete Bouguer Gravity Anomaly Map of Washington (Bonini, Hughes, and Danes, 1974), excerpted in Figure 5, show a relatively smooth and consistent gradient across the Willamette Valley and the Puget Lowland which is attributed to crustal thickening. This gradient is severely disrupted in the Portland area by a closed high centered south of Portland which extends northward through the study area to the Columbia River, and a closed low in the Tualatin Valley. The gravity high through the Portland Basin is inconsistent with the simple synclinal structure indicated by the well log data. Previous gravity work by Johnson and others (1976) and Jones (1977) modeled this gravity high as a high density intrusion possibly related to the Boring Lavas. This study attempts to define the extent of this feature in the study area.

Boring Lava

A preliminary study of the chemistry of the Boring Lava in Beeson and others (1976) revealed that different chemical types seemed to be grouped geographically. It

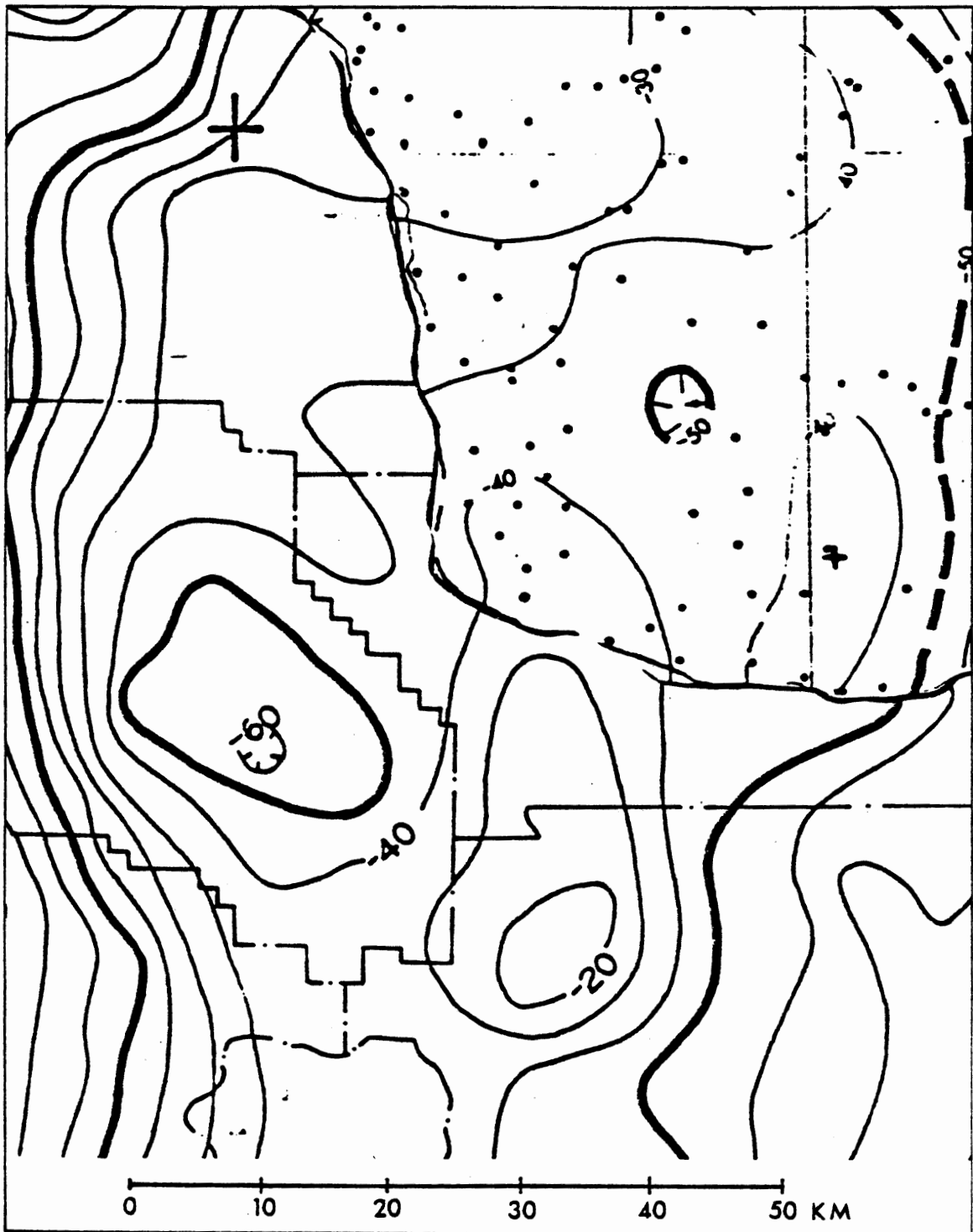


Figure 5. Complete Bouguer gravity anomaly map of Portland and vicinity, from Berg and Thiruvathukal (1967) and Bonini, Hughes and Danes (1974).

was hypothesized that the structures might control the location and chemistry of the Boring Lava vents. Northwest trends (parallel to the Portland Hills Fault) and northeast trends (parallel to the Yamhill-Bonneville Lineament) of vent locations have been noted by Allen (1975) and Beeson and others (1976). The gravity data was scanned for offsets between the vents.

Gravity values over individual Boring Lava vents were also gathered to investigate the structure of an individual vent.

GRAVITY SURVEY

Approximately 750 gravity stations are included in this survey. The author measured approximately 350 of these stations in the period 1974 to 1976. The following previous surveys comprise the remainder of the data set:

1. Schmela (1971): Gladstone Line, Milwaukie Line, Redland Line, and Transmission Line; totaling approximately 90 stations.
2. Cash (unpublished, 1973): areal survey in the northern portion of the study area; totaling approximately 100 stations.
3. Johnson, Donovan, and Moran (1976): Kings Heights-Albina Line and Sellwood Line; totaling approximately 90 stations.

4. Jones (1977): Oakgrove Line; totaling approximately 100 stations.

The distribution of stations is somewhat uneven, with an average spacing of about two stations per square kilometer, which can be compared to the average spacing of one station per 70 square kilometers west of 119 degrees longitude on the Oregon state gravity survey. In the Boring Hills in the southeast corner of the study area, coverage is limited because of the lack of elevation control and the hilly geography.

Gravity measurements in 1974 were made with a Worden gravimeter on loan from Z.F. Danes of the University of Puget Sound, and subsequent measurements were made with a Worden gravimeter on loan from Oregon State University.

Absolute gravity was transferred from the Portland International Airport base station, having a value of 980648.24 milligals (mgals , 10^{-3} cm/sec^2) to a base station at Portland State University (PSU) in 1975, having an absolute value of 980641.35 mgals . Data for drift corrections were obtained by occupying the PSU base station at the beginning and end of each day. Temporary field base stations were established in the field each day and reoccupied intermittently throughout the day. Stations measured by the author in 1974 and by Cash were subsequently tied into the PSU base station at several

points to obtain their absolute gravity values.

Most stations were located on benchmarks so resulting elevation correction errors are negligible. Elevations for the 1974 stations were taken from the United States Geological Survey (USGS) 7-1/2' quadrangles, consequently elevation estimates may be in error by as much as 3 meters, resulting in potential elevation correction errors as large as 0.6 mgals. These earlier surveys were in generally flat terrain so errors should be less than 0.3 mgals for most stations. Because several different base levels are used for benchmark surveys in the Portland area, all elevations were adjusted to the USGS 1914 Base Level. Gravity data from Johnson and others (1976) was adjusted to this base level by subtracting 1.38 feet from that survey's elevations. The resulting complete Bouguer gravity anomaly adjustment was -0.08 mgals.

DATA REDUCTION

Free-air, Bouguer, and terrain corrections were applied to all observed values, using a density of 2.67 gm/cm^3 for the material between sea level and the station elevation. Terrain corrections were calculated for 150 stations using Hammer terrain correction charts and tables in Dobrin (1976). In relatively flat areas, terrain corrections were interpolated between calculated

stations. Terrain corrections varied from 0.02 mgals to a maximum of 4.37 mgals on top of Mt. Scott, with the majority of corrections falling between 0.05 mgals and 0.2 mgals.

The theoretical gravity value for each station was calculated using the "International Gravity Formula" in Dobrin (1976). All of the above corrections with the exception of the drift corrections and terrain corrections were done using a computer for speed and accuracy. For more information on gravity surveys and data reduction, see Dobrin (1976) or Nettleton (1971).

DATA COMPILATION

Complete Bouguer Gravity Anomaly Map

Complete Bouguer anomaly values are obtained by subtracting the theoretical gravity value from the observed gravity value. These values reflect lateral density variations in the earth's crust. The complete Bouguer anomaly values in the study are contoured at a one mgal interval in Plate 1.

Several features are notable on this map. A gravity high is present in the southwest part of the study area. The high branches into a north-trending nose and a northwest-trending nose, separated by a northwest-trending linear feature. The linear feature coincides

with the Portland Hills Fault trend. The northwest-trending nose of the gravity high is well-defined for about 15 kilometers in the study area and has an amplitude of about 10 mgals. It is centered over the Willamette River near Gladstone. The north-trending nose is more poorly defined especially in the center of the study area, but appears to extend from the southern boundary of the study area to the northern boundary, a distance of nearly 30 kilometers. Because of its poor definition, the amplitude of this anomaly is difficult to estimate.

Several other features are also apparent on Plate 1. The decreasing gravity values in the eastern half of the map area reflect the regional gradient evident on Figure 5. In opposition to the regional trend, gravity decreases northwestward to -45 mgals in the northwest corner of the study area, between the Columbia and Willamette Rivers. Closed gravity lows occur over Mt. Scott and Walters Hill, both Boring Lava centers. The downwarping of the Columbia River basalt beneath the Portland Basin indicated by well logs is not apparent in the gravity data. If the basin were the only structural feature affecting the gravity, the gravity contours should mirror the structure-contours on top of the Columbia River basalt shown in Figure 4. Since this

is not the case, other structural complexities must exist.

Figure 6 is a comparison of the Complete Bouguer Gravity Anomaly Map of Oregon prepared by Berg and Thiruvathukal (1967) and data from the Complete Bouguer Gravity Anomaly Map of the Portland Basin (Plate 1). In general, the new data is consistent with the state map; however, the -20 mgal contour which outlines the northwest nose of the gravity high extends much farther north than indicated on the state map.

Residual Complete Bouguer Gravity Anomaly Map

To clarify the Bouguer anomalies caused by relatively shallow features, the gravitational effect of the east-west crustal thickening was removed from Plate 1. This was achieved by measuring the east-west distance between each station and an arbitrary longitudinal line near the western edge of the study area, then applying the appropriate correction factor. A regional gradient of approximately one mgal per kilometer was estimated from the Oregon and Washington state Bouguer anomaly maps. All values were adjusted to a zero value assigned to a station in the northwest corner of the study area on this arbitrary line. The values resulting from this operation are contoured at a one mgal interval on Plate 2, the Residual Complete Bouguer Gravity Anomaly

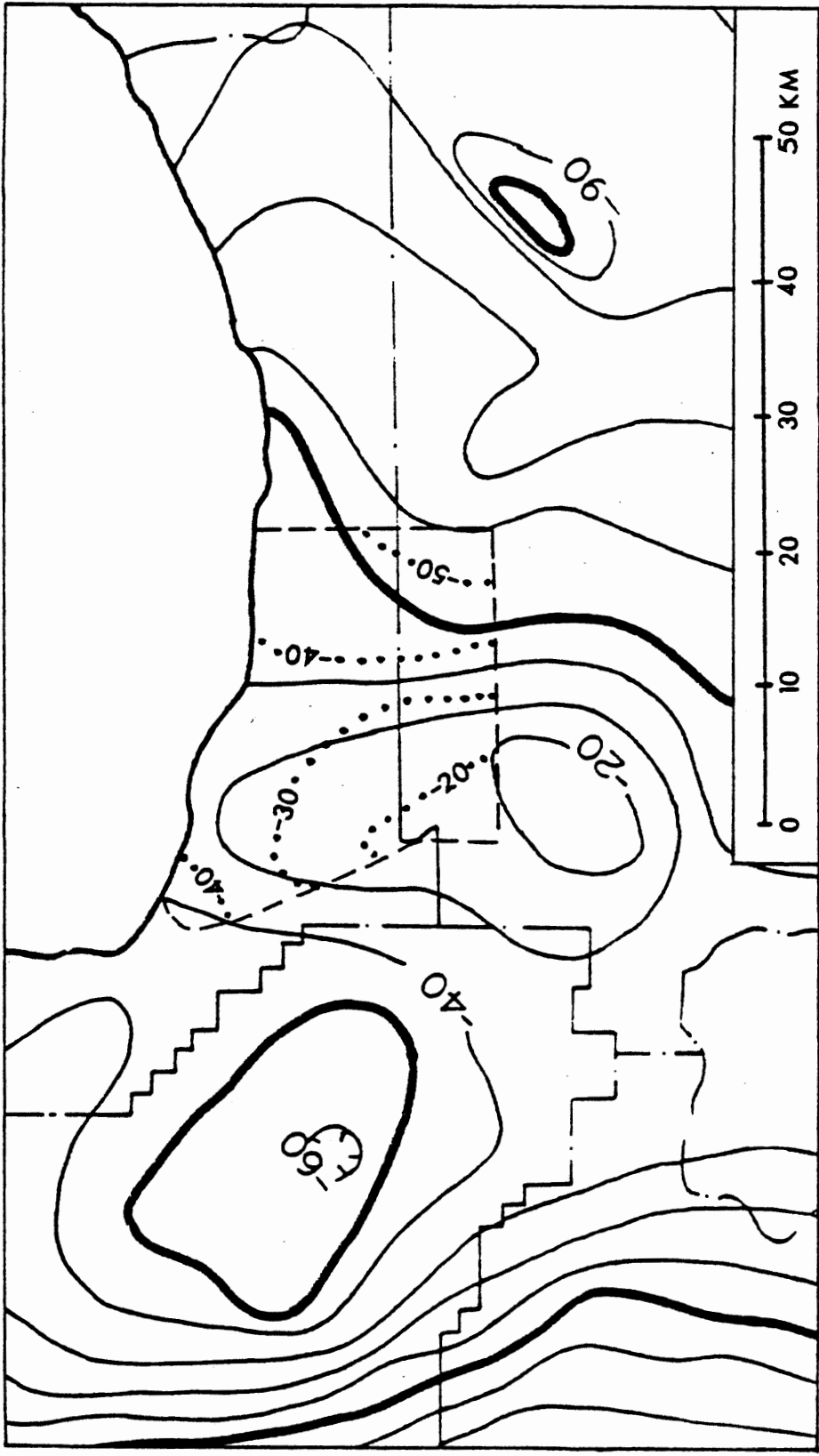


Figure 6. Comparison of the Complete Bouguer Gravity Anomaly Map of Oregon by Berg and Thiruvathukal (1967) and the Complete Bouguer Gravity Anomaly Map of the Portland Basin. Dotted lines represent data from the Complete Bouguer Anomaly Map of the Portland Basin.

Map of the Portland Basin. Plate 2 also shows the locations of the gravity models discussed in the following sections and the well locations shown on Figure 2.

The gravity high in the southwest quadrant of the study area remains the dominant feature on this map. The linear feature located along the Portland Hills Fault trend again divides the gravity high into two noses. The removal of the regional gradient accentuates the north-trending nose which has an amplitude of about 8 mgals. The northwest-trending nose of the gravity high remains very distinct with an amplitude of about 6 mgals; however its northwest-trending axis has shifted slightly eastward over Oatfield Hill rather than over the Willamette River. The gravity high continues to increase south of the study area as shown in Figure 5.

The decreasing gravity in the northwest portion of the study area has also been accentuated by the removal of the regional gradient. The state gravity map and data from the Newberry Road-Sauvie Island Line by Johnson and others (1976), located northwest of the study area, indicate that this feature is saddle-shaped and that gravity increases again about 5 km to the northwest of the 0 mgal isogal on Plate 2.

MODELING

The gravity anomalies shown on Plates 1 and 2 were analyzed by modeling four lines. The lines to be modeled were located when possible perpendicular to the feature to be modeled and through a maximum number of data points. Values were taken from the data points rather than from the contoured map to assure maximum reliability of the data. The modeled lines shown on Plate 2 are designated the Columbia Boulevard Line (A-A'), the Stark Street Line (B-B'), the Holgate Boulevard Line (C-C'), and the Clackamas Highway Line (D-D'). Previously completed models included in this report are the Kings Heights-Albina Line (E-E') and the Sellwood Line (F-F') from Johnson and others (1976) and the Oak Grove Line (G-G') from Jones (1977).

Residualized gravity values were used for modeling to avoid modeling the thickening crust at depth in each model. A correction was applied to the residual gravity values to compensate for the difference between 2.67 gm/cm³ and the actual density of the material above sea level. All modeling was done by computer methods developed by Talwani and others (1969) with adjustments of the programs to operate on PSU's computer by Ansel Johnson and Terry Jones (Jones, 1977). The models are two-dimensional with the third dimension assumed to be infinite. Ideally, the trend of a cross-sectional model

should be perpendicular to the strike of the feature to be modeled; however, some lines cross several features having different trends, so some error is inevitable.

Geologic control for the models is from well logs and previous geologic mapping in the Portland area. Densities and geologic abbreviations for the units used in modeling are shown in Table I. Densities are based on data from Bromery and Snavely (1964), R.O. Van Atta (personal communication to A. Johnson, 1975), and Z.F. Danes (personal communication to A. Johnson, 1975).

TABLE I
STRATIGRAPHIC UNITS USED IN MODELS

Stratigraphic Unit	Density gm/cm ³	Geologic Abbreviation
Post-Columbia River Basalt Sedimentary Rocks-Portland Basin	2.3	QTs ₁
Post-Columbia River Basalt Sedimentary Rocks-Tualatin Valley	2.0	QTs ₂
Boring Lava	2.5	QTb
Intrusive Rocks	3.0*	QTi
Columbia River Basalt Group	2.8	Tcrb
Late Eocene to Oligocene Sedimentary Rocks	2.4	Toes
Skamania Volcanic Series	2.8	Tsv
Eocene Sedimentary Rocks	2.5	Tes
Siletz River Volcanic Series	2.8	Tsrv

*In one model, 3.1 gm/cm³ was used.

The following models represent geologic interpretations which appear to best fit the gravity data based on the existing geologic data. The models are not intended to represent unique solutions, but do provide quantitative estimates of the densities, sizes, and shapes of features interpreted to be causing the anomalies. For ease of computation, the shapes of the blocks used in modeling are simplifications of the proposed geologic features. For instance the contact between the Skamania Volcanics and the Eocene and late Eocene to Oligocene sedimentary rocks is shown as a straight line, when in fact, a great deal of interfingering undoubtedly occurs as shown in Figure 3.

Each model shows the topography along the line, the observed (residualized) gravity, and the computed gravity, as well as the final gravity model. The observed gravity is shown as a solid line where detailed data is available and as a dashed line where the data source is the state map. The locations of deep wells used for stratigraphic control are also shown. Many shallower wells were also used as control but are not shown. The model used for computation extended about 70 km beyond each end of the model shown in the text to eliminate end effects. The models are drawn at a 2:1 vertical exaggeration and extend about 35 km laterally and 6 km vertically.

Columbia Boulevard Line A-A'

The Columbia Boulevard Line (A-A') parallels the Columbia River for about 24 km, from the Willamette River eastward across the northern edge of the study area. Plate 2 shows the line crossing the gravity low in the northwest corner of the study area and the northern edge of the north-trending nose of the gravity high.

Figure 7 and 8, the Columbia Boulevard 1 and Columbia Boulevard 2 models respectively, show two models which fit the gravity data. The western end of the model is located in the Portland Hills, which have an elevation of about 300 meters in this area. After crossing the Willamette River, the topography is very flat across East Portland to the east end of the line.

The observed Bouguer gravity profile shows gravity values increasing from a low of -8 mgals at the western edge of the profile to 26 mgals near 82nd Avenue. Here the profile flattens, then increases gradually to its eastern edge. There are no abrupt changes in slope which might suggest faulting in the Columbia River basalt. This gravity profile does not reflect the synclinal fold in the Columbia River basalt which is indicated by well logs, and the broad wavelength of the anomaly suggests a deeper feature.

The model in Figure 7 shows the Columbia River basalt (Tcrb) approximately 250 m (800 ft) thick, dipping

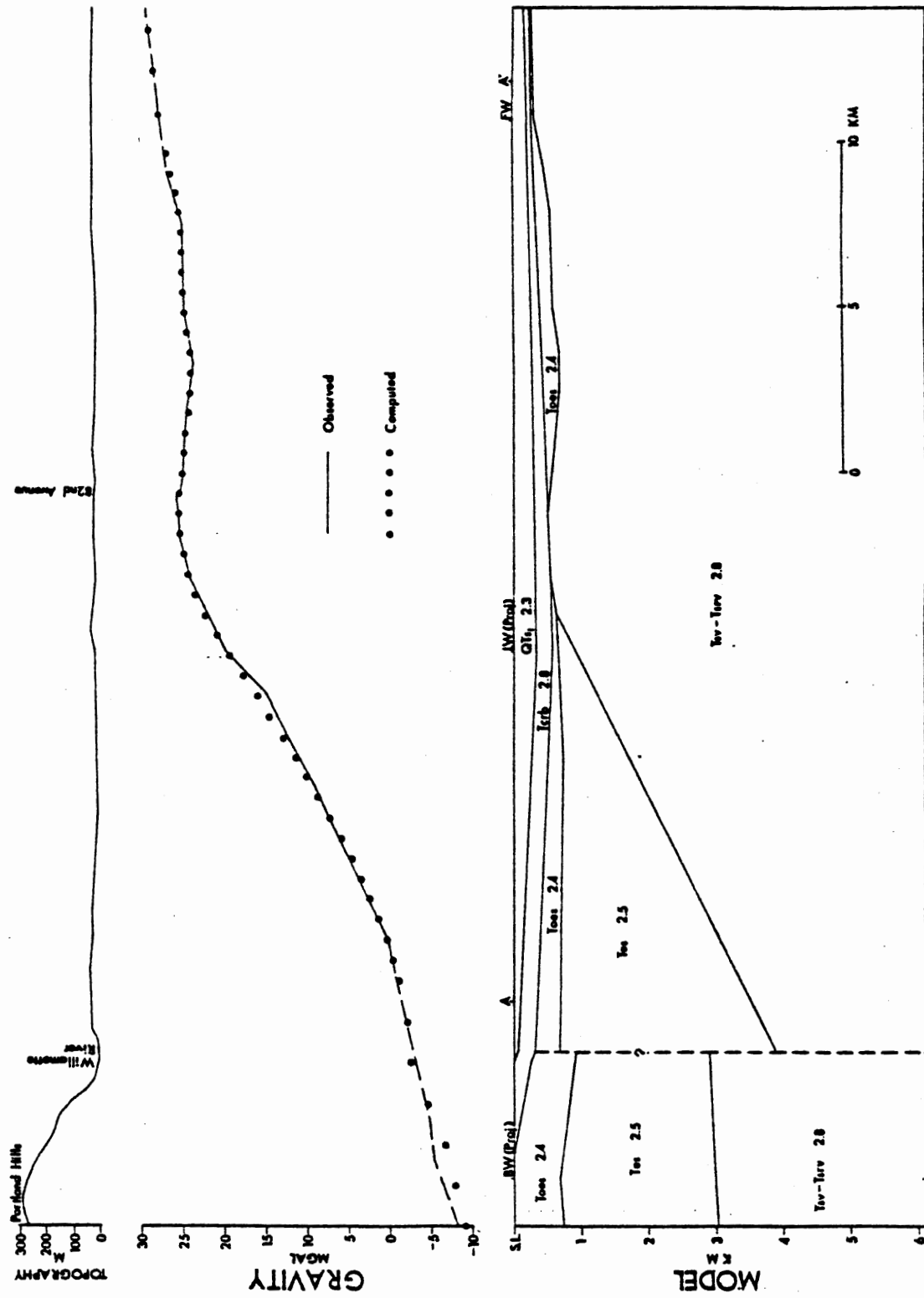


Figure 7. Columbia Boulevard 1 gravity model.

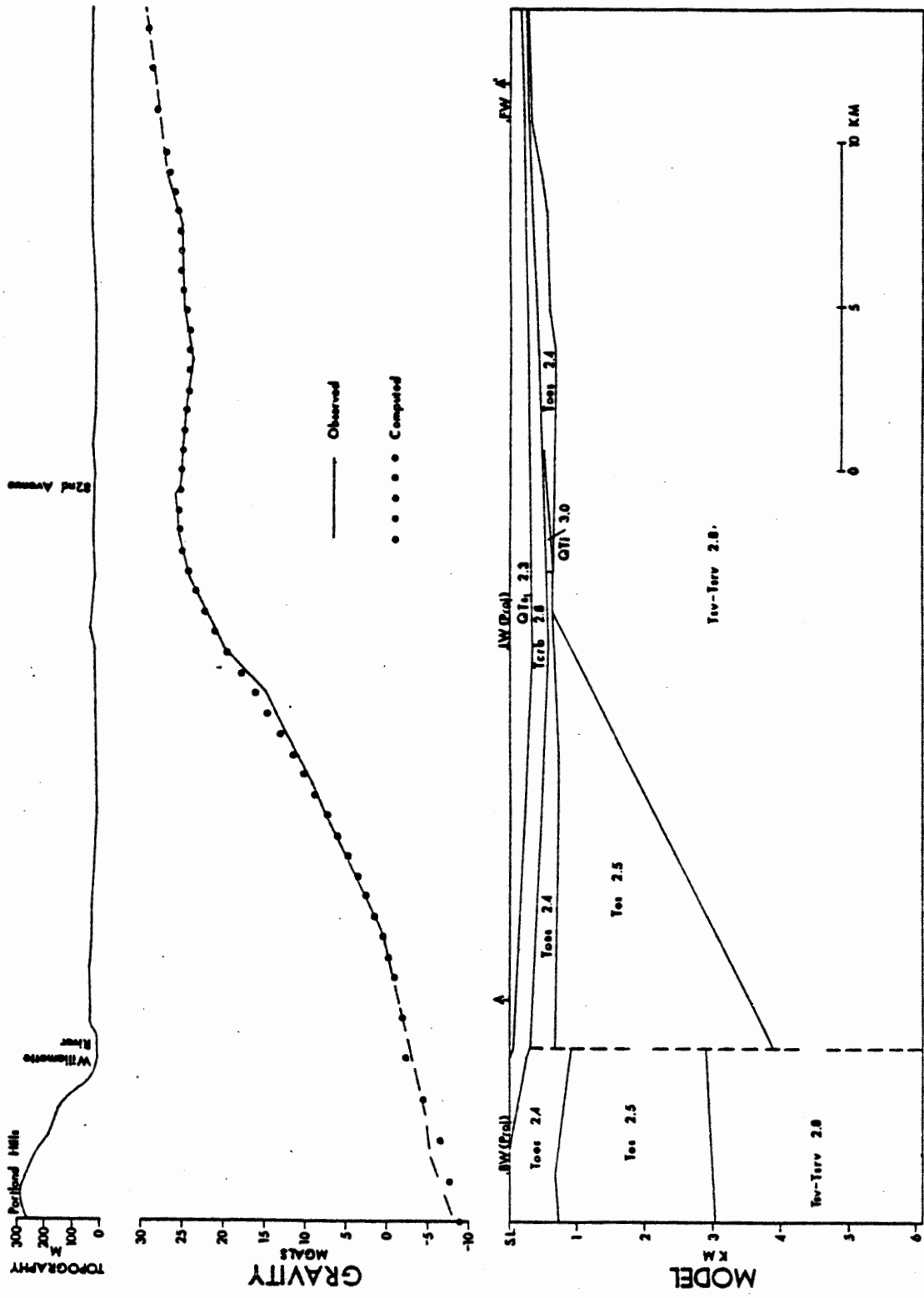


Figure 8. Columbia Boulevard 2 gravity model.

eastward into the Portland Basin from the Portland Hills. At the center of the basin, the top of the basalt is located at about -335 m (-1100 ft) elevation as projected from the Ladd well (LW). East of the Ladd well projection, the top of the Columbia River basalt slopes gently upward, and the basalt thins to 45 m (150 ft) as indicated by the Fairview well (FW). Because of the lack of detailed gravity data west of the Willamette River, no offset in the Columbia River basalt is shown on the east side of the Portland Hills along the trend of the Portland Hills Fault.

The Fairview well (FW) intercepts sedimentary rocks interpreted to be late Eocene to Oligocene age (Toes) beneath the Columbia River basalt. Their distribution east of 82nd Avenue in the model is controlled by the slight gravity decrease east of 82nd Avenue and is somewhat arbitrary due to the lack of additional wells.

The increase in gravity from the Portland Hills to 82nd Avenue may be caused by the thinning of late Eocene to Oligocene sedimentary rocks (Toes) and Eocene sedimentary rocks (Tes) against a wedge of Skamania Volcanics (Tsv). The large density contrast between these units enables an accurate location of the interface from the gravity data. It is interesting to note, that models south of the Columbia Boulevard Line constructed for this study and models constructed for previous studies have all

located the "sediment-volcanic interface" west of the Willamette River beneath the Portland Hills. When stratigraphic limits from the Barber well (BW) are projected north-northwest along the structural trend of the Portland Hills onto A-A', computed gravity values are substantially too high. This well encountered about 730 m (2400 ft) of late Eocene to Oligocene sedimentary rocks and 180 m (600 ft) of Eocene sedimentary rocks, placing the top of the Skamania Volcanics at about -850 m (-2800 ft). To accommodate the decreasing gravity across the Portland Hills, this model shows the thickness of the Eocene sedimentary rocks increasing to over 2000 m (6560 ft).

The fault on the east side of the Portland Hills is not essential for agreement with the observed gravity values. Major displacement on the fault is interpreted to be right-lateral. The vertical discrepancies in stratigraphic thicknesses across the fault could be halved and continuous contacts drawn without changing the computed values appreciably. The fault is included here as a possible structural solution to the apparent displacement of the "sediment-volcanic interface" which will be discussed later.

The Columbia Boulevard 2 model shown in Figure 8 differs from Figure 7 only in that a small intrusive

body (QTi) lies beneath the Columbia River basalt in the vicinity of 82nd Avenue. It is included as an alternate interpretation here because intrusions occur in all models which cross the north-trending nose of the gravity high south of A-A'. Since this line can be modeled without an intrusion, this area may be close to the northern extent of the intrusive body.

Stark Street Line B-B'

The Stark Street Line (B-B') runs east-west from the Willamette River to the Sandy River as shown on Plate 2. The line lies south of the gravity low in the northwest corner of the study area and north of the northwest-trending nose of the gravity high, but crosses a broad section of the north-trending gravity high.

Figure 9, 10 and 11 show models for this line. With the exception of the Portland Hills and the northern flank of Mt. Tabor, shown just west of 82nd Avenue, the topography is quite flat. The gravity profile shows gravity increasing rapidly from a low of -4 mgals at the western edge of the profile to 25 mgals near the Willamette River. Eastward, values continue to increase but much more gradually to Mt. Tabor. East of 82nd Avenue values begin to drop slightly, then gradually increase again further east. As with the Columbia Boulevard Line, the observed gravity profile does not reflect the shallow

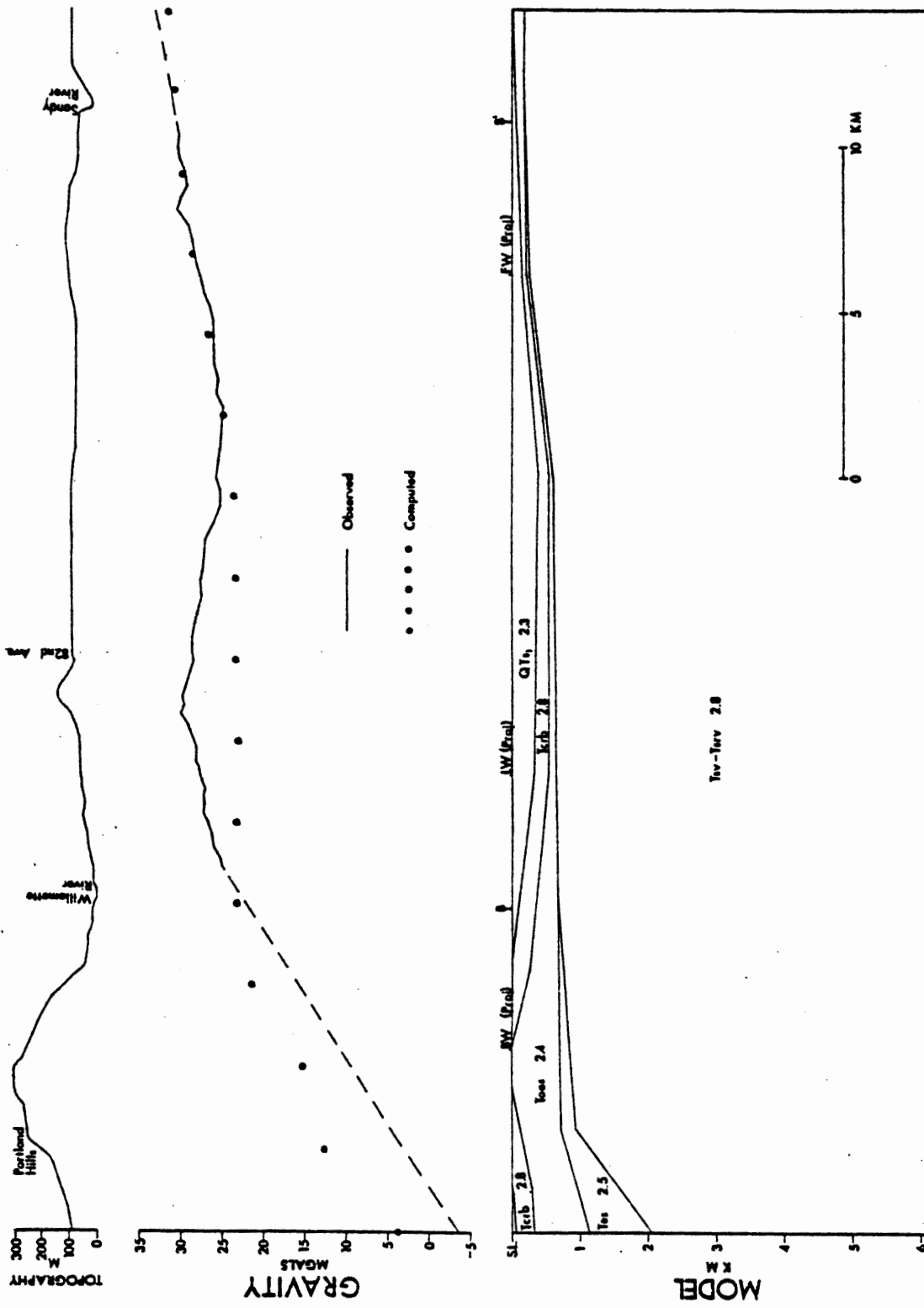


Figure 9. Stark Street 1 gravity model.

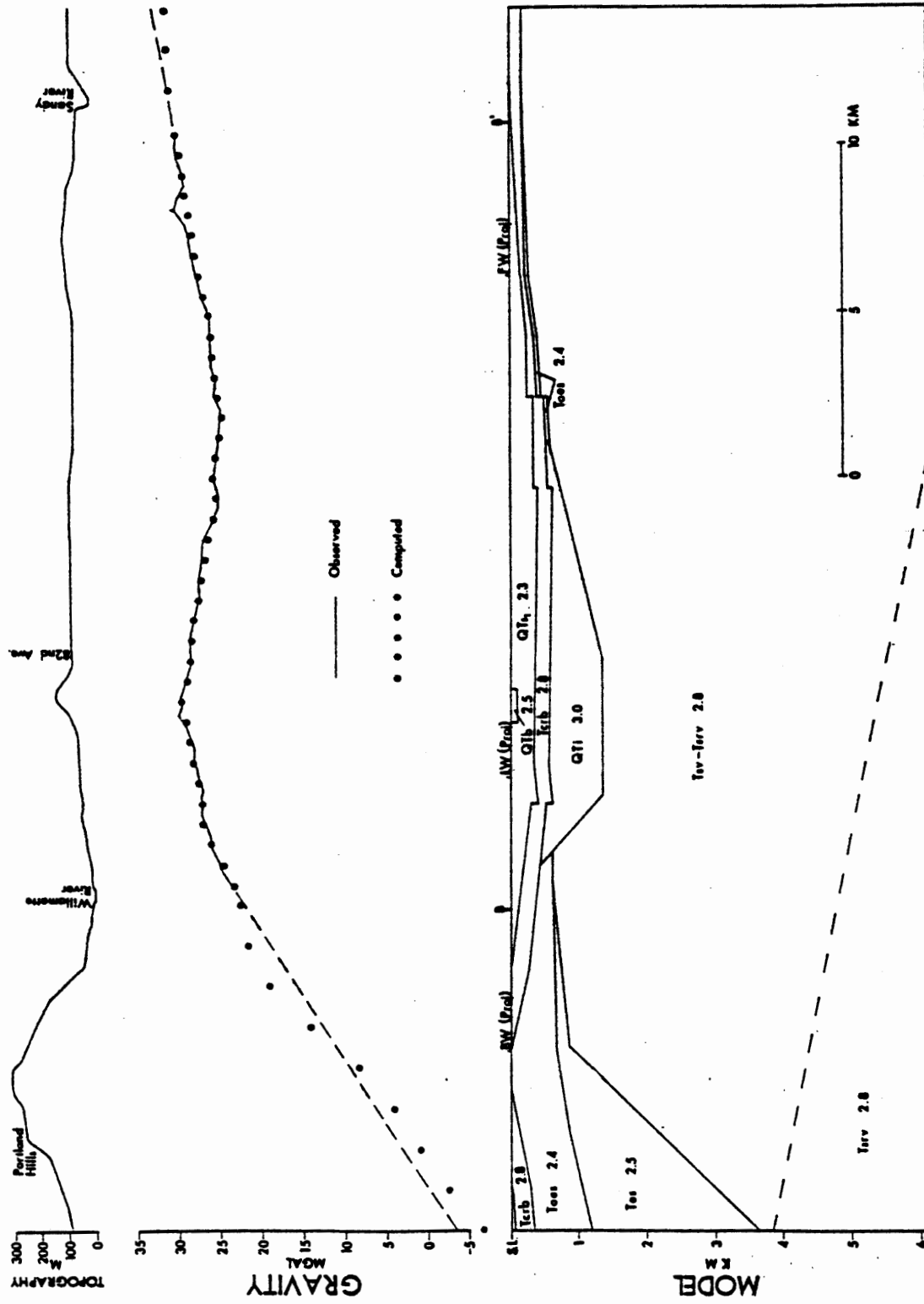


Figure 10. Stark Street 2 gravity model.

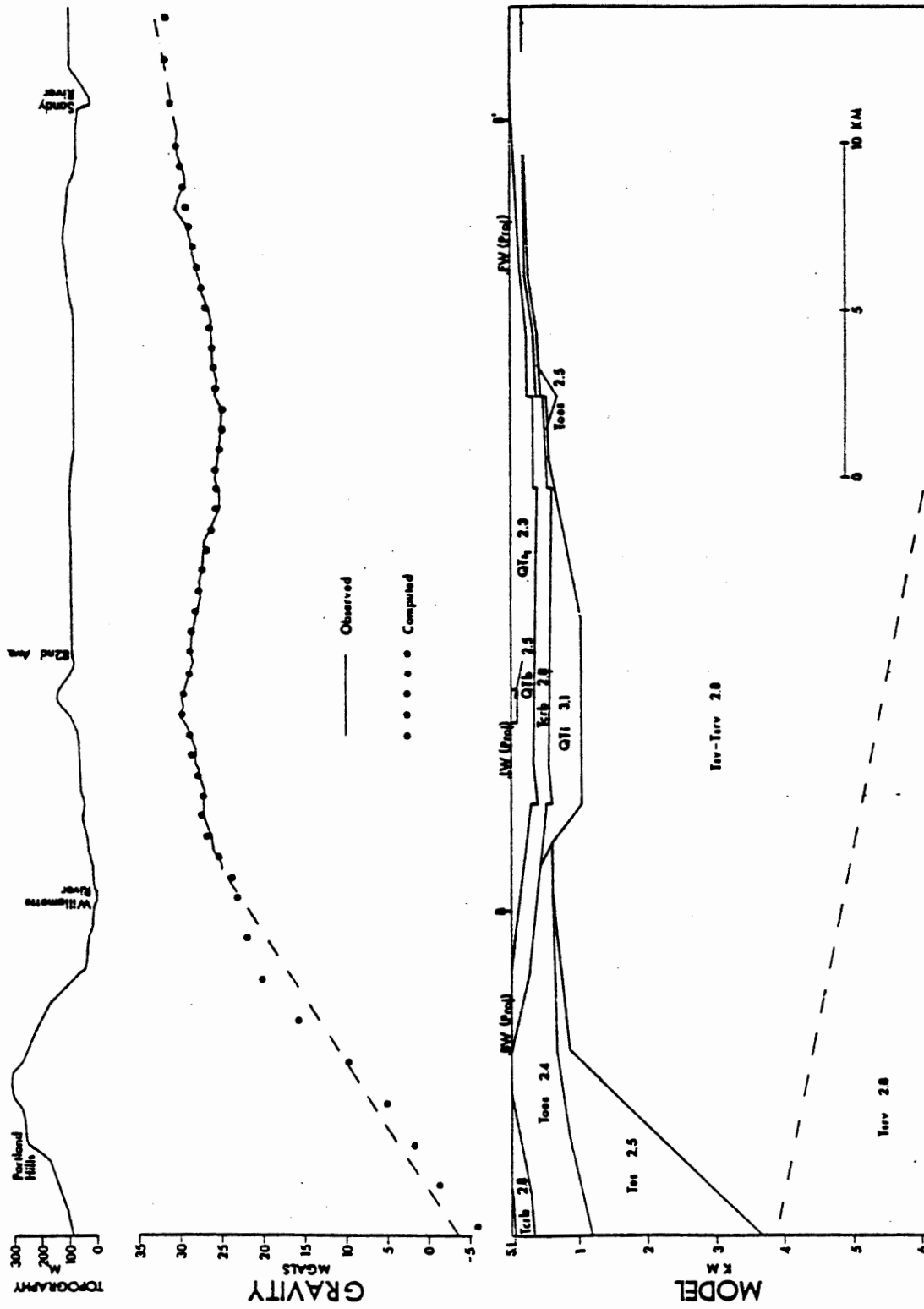


Figure 11. Stark Street 3 gravity model.

synclinal structure of the Portland Basin and must be the result of a deeper structure. Small changes in slope superimposed on the gravity high may reflect structures in the Columbia River basalt.

The Stark Street 1 model, Figure 9, shows a simplified model that is consistent with the well log and outcrop data. The primary features of the model are the Columbia River basalt (Tcrb), 260 m (850 ft) thick, anticlinally folded in the Portland Hills and synclinally folded beneath the Portland Basin. The Columbia River basalt thins on the east limb of the syncline as required by the Fairview well (FW). The late Eocene to Oligocene sedimentary rocks thin gradually to the east over the Skamania Volcanics (Tsv), pinching out entirely at the Sandy River. The Eocene sedimentary rocks thin abruptly to the east against the Skamania Volcanics beneath the Portland Hills as interpreted in the cross-section by Newton (1969) shown in Figure 3. As can be seen in Figure 9, the computer gravity values from this model are not in agreement with the observed gravity values. A positive residual of approximately 6 mgals remains in the 82nd Avenue area, and a negative residual of from 5 to 10 mgals remains at the western edge of the profile.

The location of the positive residual anomaly in Figure 9 corresponds to the north-trending gravity high on Plate 2. Replacing the late Eocene to Oligocene sedimentary rocks with Skamania Volcanics in the vicinity of 82nd Avenue did not raise the computed gravity values substantially. The Ladd well (LW) requires about 350 m (1100 ft) of post-Columbia River Basalt sedimentary rocks in the vicinity of the well, consequently increasing the thickness of the Columbia River basalt at the expense of the overlying sedimentary rocks is not an acceptable interpretation for increasing the computed gravity values. This positive anomaly must be due to a feature beneath the Columbia River basalt which has a density greater than 2.8 gm/cm^3 , the density of the Columbia River basalt and the Skamania Volcanics. No wells penetrate the Columbia River basalt in this area, so the nature of the feature causing the gravity high is speculative. Previously completed models by Johnson and others (1976) and Jones (1977) south of the Stark Street Line which cross the gravity high have interpreted the gravity high as an intrusion having a density of 3.0 gm/cm^3 .

The Stark Street 2 model, shown in Figure 10, succeeds in gaining agreement between the computed and observed gravity values by incorporating an intrusion. In this model, the Columbia River basalt is folded in the Portland Hills and under the Portland Basin, and thins to the east

as in Figure 9. In addition, minor faults having offsets ranging from about 30 to 60 meters in the Columbia River basalt are shown. The presence of these faults is based only on minor variations in the observed gravity data, and therefore should be viewed as hypothetical. Well logs which intersect the Columbia River basalt in this area are too few to substantiate or disprove these structures. The dip on all faults is assumed to be vertical. The structures shown in the Columbia River basalt form a graben structure beneath the Portland Basin with a slight upward bowing in the Columbia River basalt beneath Mt. Tabor.

Because detailed data is not available west of the Willamette River, the degree of agreement sought in this part of the model is considerably less than in the rest of the gravity line. The computed gravity values shown in Figure 9 suggest that the "sediment-volcanic interface" must be steeper and that the sedimentary wedge must extend farther east than shown in that model. The contact shown in Figure 10 slopes about 30 degrees and yields computed values which roughly agree with the observed values. The stratigraphic thicknesses at the top of the slope are based on projections of the Barber well (BW) data. Adjustments in these contacts would allow a closer correlation between observed and computed values, however the degree of uncertainty in the observed gravity values west of the Willamette is as large as these residuals.

In the Stark Street 2 model, a sill-shaped intrusion (QT_i) having a density of 3.0 gm/cm³ is located beneath the Columbia River basalt in the center of the line. The intrusion is approximately 12,200 m (40,000 ft) wide and 730 m (2,400 ft) thick at its thickest point. The dimensions of the intrusion are somewhat arbitrary because, as with any gravity model, a number of solutions would produce agreement.

After modeling the gravity high with the intrusion, a small positive residual remained beneath Mt. Tabor, whose northern flank is shown on the topographic profile just west of 82nd Avenue. Since Mt. Tabor is a Boring Lava vent, a Boring Lava plug having a density of 2.5 gm/cm³ was included in the model to account for the residual.

To investigate the consequences of varying the density of the intrusion, the Stark Street 3 model was developed using 3.1 gm/cm³ as the assumed density of the intrusion. This model is shown in Figure 11. Other parts of the model are identical to Figure 10. This density value is considered an upper limit for rock types than might occur in this area. As can be seen on the model, the general shape of the intrusion is very similar to that shown in Figure 10. The primary difference is the thickness which decreases to 490 m (1600 ft), while the lateral extent remains the same.

Holgate Boulevard Line C-C'

The Holgate Boulevard Line (C-C') runs east-west about 3 km south of the Stark Street Line. As shown on Plate 2, it crosses the north-trending nose of the gravity high and appears to cross the Willamette River and the Portland Hills north of where the northwest-trending nose of the gravity high becomes a dominant feature. The eastern portion crosses a gentle gravity low.

Figure 12 and 13 show the Holgate Boulevard 1 and Holgate Boulevard 2 models respectively. The topography is relatively flat along the line except in the Portland Hills. Gravity values increase from a low of -5 mgals at the western edge of the line to about 30 mgals at the Willamette River. From the Willamette River to about 82nd Avenue, the gravity increases gradually to about 32 mgals and then decreases to 24 mgals about 7 km east of 82nd Avenue. Near the eastern edge of the detailed line, shown as a solid line on the observed gravity profile, a 3 mgal increase may represent faulting in the Columbia River basalt.

The Holgate Boulevard 1 model shown in Figure 12 includes many of the same features shown on the Stark Street models. Folds in the Columbia River basalt form the Portland Hills and the Portland Basin. The thickness of the Columbia River basalt decreases from 250 m (800 ft)

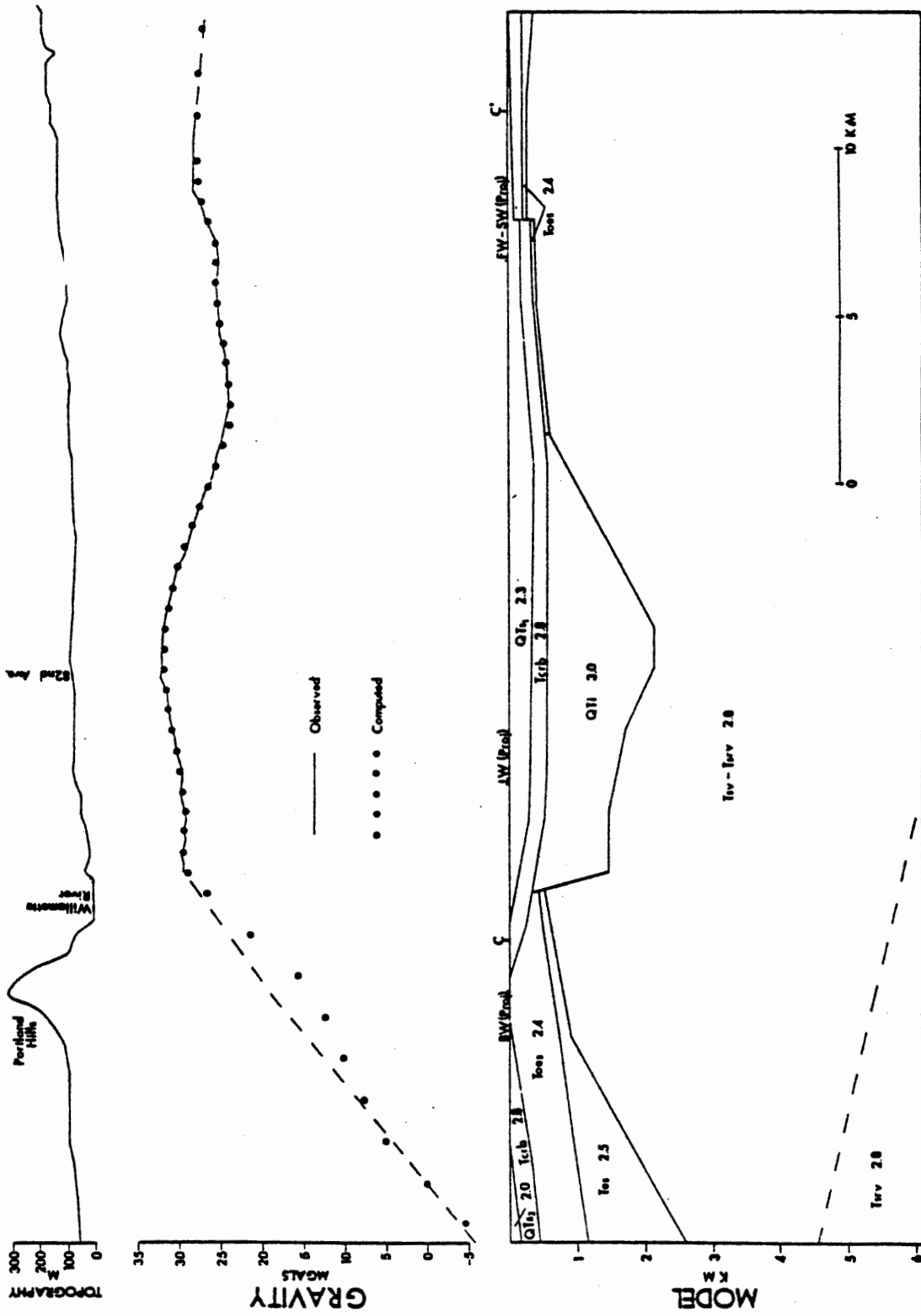


Figure 12. Holgate Boulevard 1 gravity model.

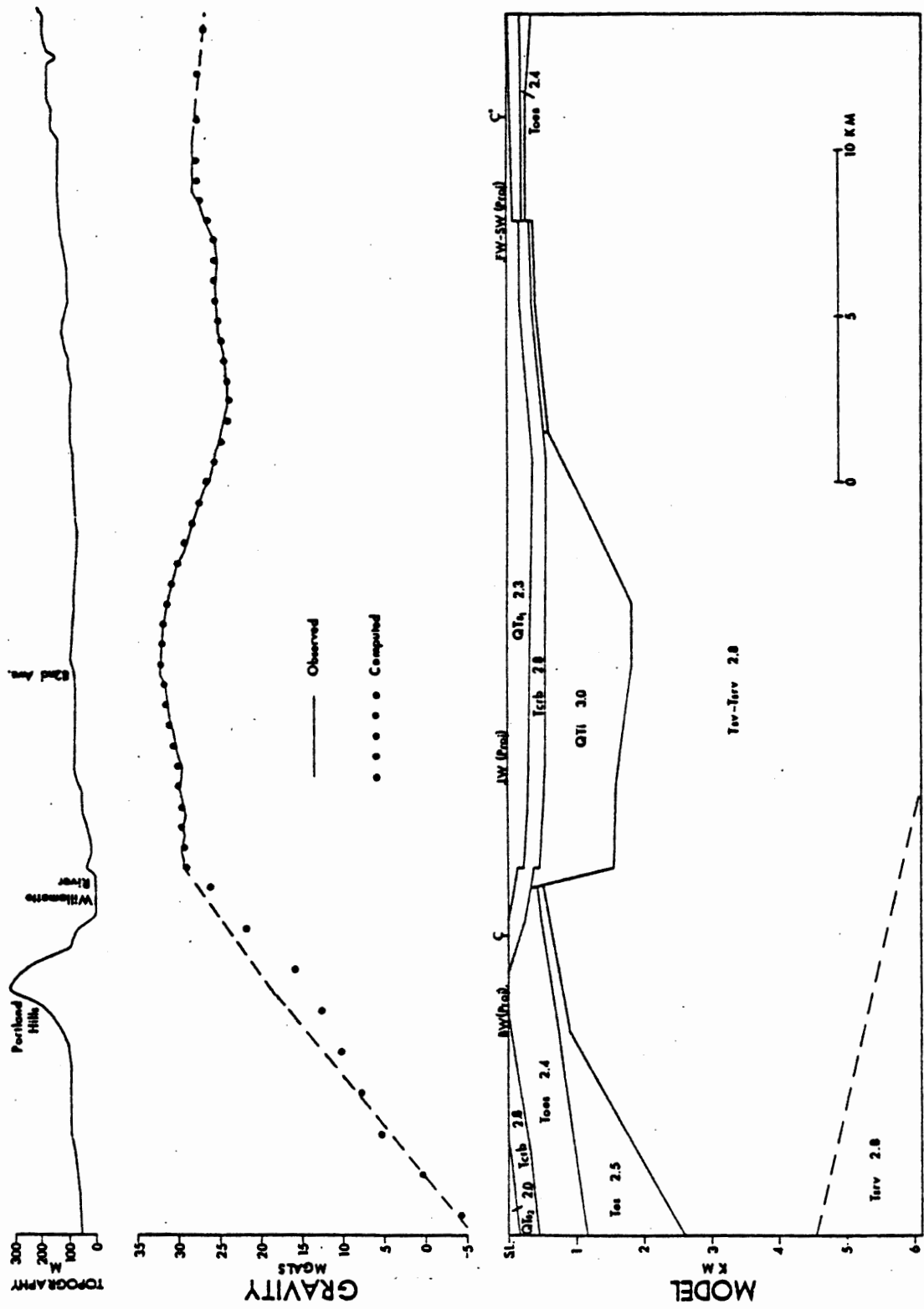


Figure 13. Holgate Boulevard 2 gravity model.

beneath the Portland Hills and the western half of the Portland Basin to 150 m (500 ft) near the eastern edge of the line. The 3 mgal gravity increase approximately 14 km east of 82nd Avenue is modeled with a vertical fault having an offset, up to the east, of approximately 90 m (300 ft). Projections between the Fairview (FW) and Shiiki (SW) wells define the elevation of the top of the Columbia River basalt on the down-dropped side of this fault with some accuracy, but no other wells in the area aid in further defining this structure, so its existence is somewhat questionable. No faulting along the Portland Hills Fault trend is necessary to fit the gravity data, however, detailed data were not collected west of the Willamette River, so faulting along the trend is not precluded.

The "sediment-volcanic interface" is a predominant feature on this model as in previous ones. The change in slope of the contact occurs beneath the Portland Hills with the steeper contact dipping about 13 degrees west.

An intrusion is again necessary to account for the amplitude of the gravity high near the center of the line. In this model, the intrusion is larger than the intrusion in the Stark Street Line, having an average width of about 13,400 m (44,000 ft) and an average thickness of 1,340 m (4,400 ft).

Figure 13 shows the Holgate Boulevard 2 model. In this model, the shape of the intrusion is simplified giving it a more uniform thickness. To offset the added mass in the western part of the intrusion, a vertical fault displaces the Columbia River basalt 90 m (300 ft) down to the east. This fault is not substantiated or disproved by the existing well log data, so either model is acceptable.

Clackamas Highway Line D-D'

The southernmost line modeled for this study is the Clackamas Highway Line (D-D') which runs roughly east-west near the southern boundary of the study area. As shown on Plate 2, this traverse crosses both the north- and northwest-trending noses of the gravity high and the steep gradient across the Portland Hills Fault trend which separates the noses. Gravity values decrease to the eastern edge of the line.

Figure 14 shows the Clackamas Highway model. The model begins west of the Portland Hills, crosses the Willamette River, Oatfield Hill, and 82nd Avenue, then crosses the Boring Hills. Although the Portland Hills are more subdued than in traverses further to the north, the topography along the rest of the line is much more variable than on previous lines.

The gravity profile shows values increasing very rapidly from 13 mgals at the western boundary to 40 mgals

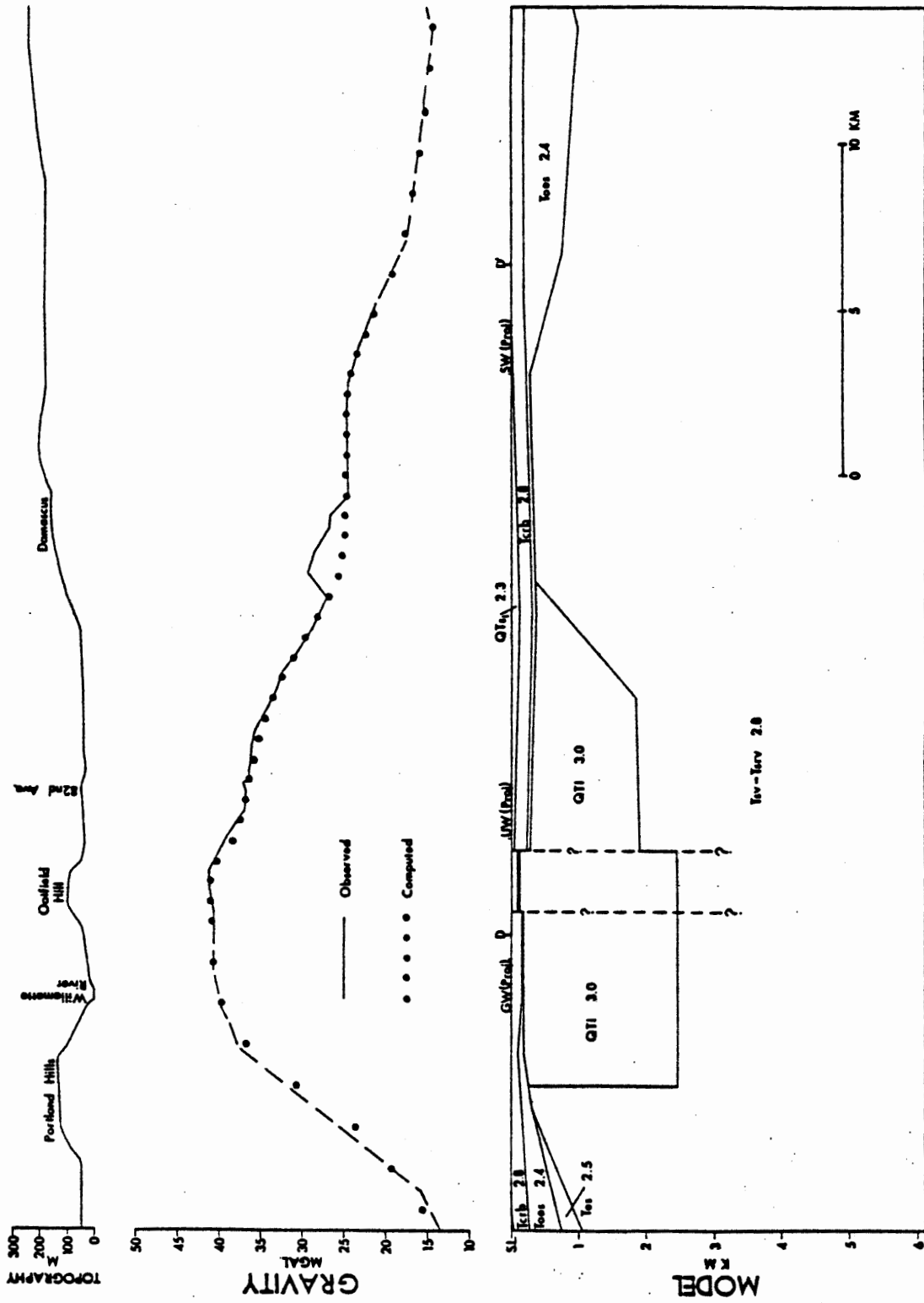


Figure 14. Clackamas Highway gravity model.

near the Willamette River. Values remain relatively constant to the eastern slope of Oatfield Hill, then begin to decrease gradually. Near Damascus a 3 mgal positive anomaly disrupts the decreasing gravity trend; however to the east of this feature values continue to decrease.

South of the line, the Gladstone well (GW) penetrates 180 m (590 ft) of Columbia River basalt before intercepting older rocks. This thickness is maintained in Figure 14 across the gentle anticlinal fold in the Portland Hills and the gentle syncline beneath the Portland Basin. Wells along this line indicate very shallow depths to the top of the basalt in comparison to areas further north as illustrated in this model. Faults offset the Columbia River basalt on both sides of Oatfield Hill. The locations of these faults are based on the detailed field mapping and geochemical correlations described in Beeson and others (1976). Figure 14 models the fault on the west side of Oatfield Hill, named the Oak Grove Fault by Beeson and others (1976), with an offset of 60 m (200 ft), down to the west. The fault on the east side of Oatfield Hill is correlated with the Portland Hills Fault and is modeled with an offset of 120 m (400 ft), down to the east. The vertical location of the Columbia River basalt east of the Portland Hills

Fault is controlled by the Union High School well (UW). Beeson and others (1976) suggest offsets on the Portland Hills Fault of up to 200 m (650 ft). Jones (1977) modeled this feature just north of D-D' with 300 m (980 ft) of vertical offset.

The "sediment-volcanic interface" is shown at the western edge of the Clackamas Highway model. It occurs beneath the Portland Hills and slopes about 11 degrees to the west.

The Gladstone well (GW) indicates that late Eocene to Oligocene sedimentary rocks (Toes) are present beneath the Columbia River basalt. They are modeled 30 to 60 m (100 to 200 ft) thick from the Portland Hills through the basin to the projected location of the Shiiki well (SW). The continuing decline in gravity values in the eastern part of the line is modeled as a basin filled with late Eocene to Oligocene sedimentary rocks. Wells in this area intersect the top of the Columbia River basalt near sea level, so the cause of the declining gravity is beneath the Columbia River basalt and the material must have a density less than 2.8 gm/cm^3 . No wells penetrate the base of the Columbia River basalt in this area to clarify the nature of this material.

The gravity high centered beneath Oatfield Hill is modeled with an intrusion having a density of 3.0 gm/cm^3 as in previous models. As seen on Plate 2, the Clackamas Highway Line (D-D') crosses both the north and northwest trends of the gravity high. The gradient across the Portland Hills Fault trend is greater than can be accounted for by the down-faulting of the Columbia River basalt. To satisfy the remaining anomaly, the intrusion is thicker west of the Portland Hills Fault than east of it. The thickness in the western part is about 2300 m (7600 ft) and in the eastern part about 1500 m (5000 ft). The total lateral extent is about 15,200 m (50,000 ft). In comparison to previous models, the intrusion is both thicker and wider.

PREVIOUS MODELS

Three additional gravity models which are partially located within the study area are included here. They include the Kings Heights-Albina Line (E-E') and the Sellwood Line (F-F') by Johnson and others (1976) and the Oak Grove Line (G-G') from Jones (1977). These models were developed independently from the models developed for this study. The locations of these lines are shown on Plate 2. A brief description of these models follows.

Kings Heights-Albina Line, E-E'

Figure 15 shows the Kings Heights-Albina Line (E-E') topography, gravity profile, and two models. The predominant feature on the gravity profile is the broad gravity high east of the Tualatin Mountains (Portland Hills). Model A shows nearly 500 m of offset on the Portland Hills Fault and 180 m of offset on a fault 2700 m to the east in the nearly flat Columbia River basalt (CRB). Model B, which is preferred by the authors, shows offsets of 150 m on both faults in dipping Columbia River basalt. Both models show the "sediment-volcanic interface" beneath the Portland Hills. No intrusion is necessary in this model.

Sellwood Line, F-F'

Figure 16 shows the topography, gravity profile, and model for the Sellwood Line (F-F'). The predominant feature on the gravity profile is the narrow gravity high centered over the Willamette River. The model shows the "sediment-volcanic interface" at the eastern edge of the Portland Hills. The narrow gravity high is modeled with an intrusion located directly beneath the Columbia River basalt, having a density of 3.0 gm/cm^3 . It is approximately 1500 m wide and 2800 m thick. A possible fault is shown on the east side of the intrusion, because of the sharp slope on the east side of the gravity high, which requires a near surface density discontinuity.

SELLWOOD GRAVITY MODEL

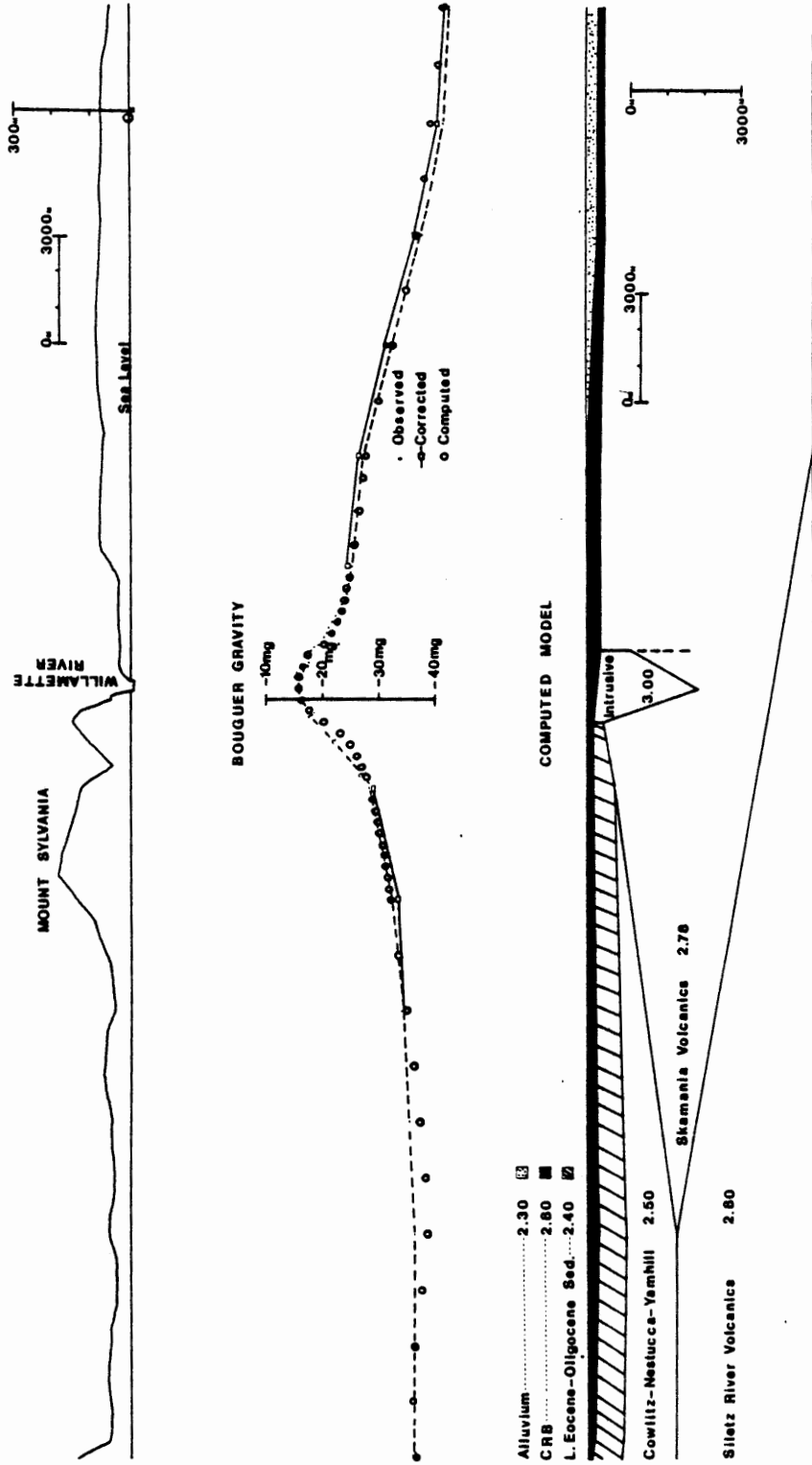


Figure 16. Sellwood Line gravity model.

Oak Grove Line, G-G'

Figure 17 shows the topography, gravity profile, and model of the Oak Grove Line (G-G'). The predominant features of the gravity profile are the broad gravity high across most of the profile and the abrupt gravity decrease east of Oatfield Hill along the Portland Hills Fault trend. The model shows an offset of 300 m down to the east along the Portland Hills Fault in the Columbia River basalt. Another fault farther to the east, offsets the Columbia River basalt 50 m down to the west. The "sediment-volcanic interface" occurs under the Tualatin River. The broad gravity high is modeled as an intrusion having a density of 3.0 gm/cm^3 . In the model, the Portland Hills Fault divides this intrusion into a thicker western portion (1350 m) and a thinner eastern portion (1100 m). The combined width of the intrusions is approximately 17,000 m.

AREAL COMPILATION OF GRAVITY MODELS

The models previously discussed have many features in common. Features which occur in several models include:

1. Structures in the Columbia River basalt
2. An Eocene to Oligocene "sediment-volcanic interface"
3. A high density intrusion.

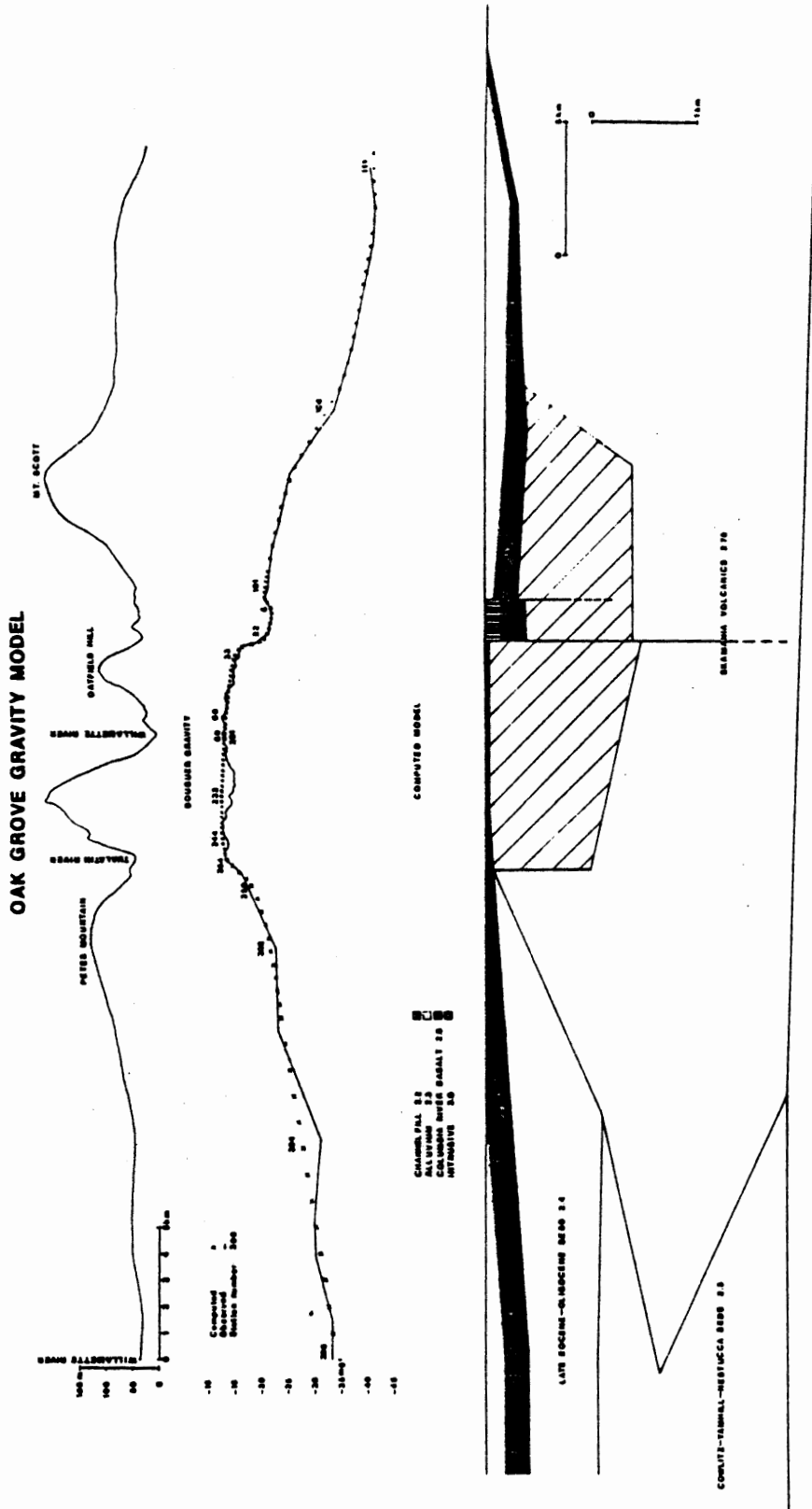


Figure 17. Oak Grove Line gravity model.

Characteristics of these features from each model are plotted on Figure 18.

Structures in the Columbia River basalt

One of the primary objectives of this study was to provide additional information on structures in the Portland Basin in the Columbia River basalt. Unfortunately, the intrusion centered over the basin tends to obscure structures in the Columbia River basalt which would be reflected in the gravity. The position of the top of the Columbia River basalt for modeling purposes is based on well log data in the area. In no instance did the gravity data contradict a well controlled depth to the Columbia River basalt. All gravity models depict synclines with very broad bottoms beneath the Portland Basin. The approximate axial trend of the syncline, shown on Figure 18, roughly parallels the Portland Hills trend and plunges northward.

Vertical faulting in the Columbia River basalt is modeled at abrupt, small wavelength, changes in gravity values. These faults are plotted on Figure 18 as short, heavy lines. With the exception of the faults located along the Portland Hills Fault (PHF) trend, the faults do not appear to define any continuous trends. Except for the Clackamas Highway Line, offsets on the Portland Hills Fault are not included in models developed for this study, although they may exist. Gravity values from

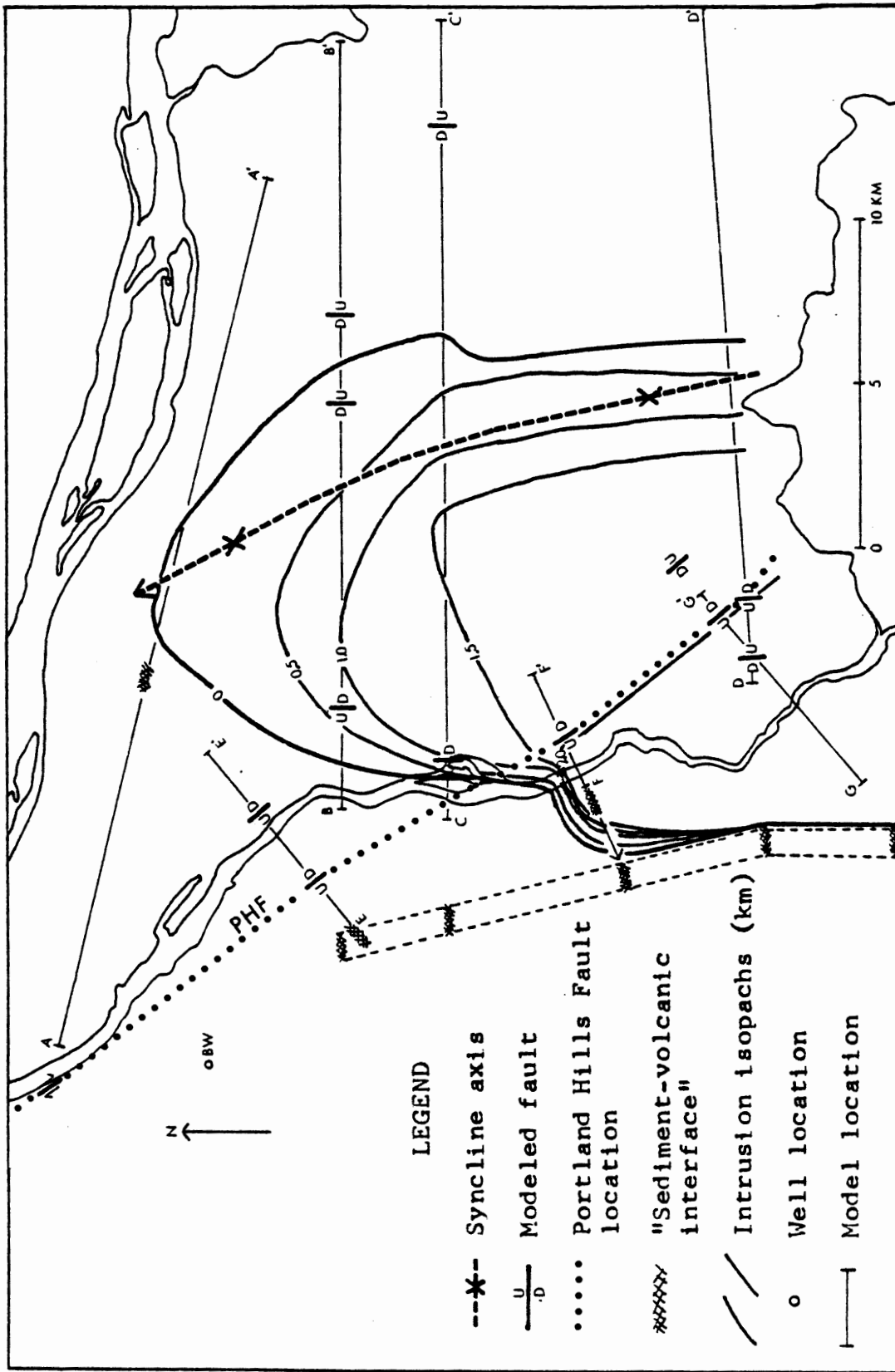


Figure 18. Gravity model compilation.

the Complete Bouguer Gravity Anomaly Map of Oregon (Berg and Thiruvathukal, 1967) used to extend the gravity lines west of the Willamette River did not require offsets in the Columbia River basalt. All faults on the west limb of the syncline, except for one fault on the Oak Grove Line, have offsets which are down to the east and the reverse is true on the east limb of the syncline. Offsets range from 30 m to 300 m.

Eocene to Oligocene "sediment-volcanic interface"

Near the western edge of each line, gravity values decrease abruptly. This has been modeled by thinning the Eocene sedimentary rocks and late Eocene to Oligocene sedimentary rocks against the Skamania Volcanics. This contact has been named the "sediment-volcanic interface". Where the gravity values begin to decrease, the dip of the modeled interface changes from nearly flat to 11 to 30 degrees to the west. The location of the change in slope of the sediment-volcanic interface from each model is plotted on Figure 18 as a hatched zone. The location of the "sediment-volcanic interface" from the Sellwood Line (F-F') has been adjusted westward as shown by the arrow in Figure 18. It appears that if the data from this study had been available when the Sellwood Line was modeled, gravity values west of the western end of the line would have been higher than the values derived from

the Complete Bouguer Gravity Anomaly Map of Oregon (Berg and Thiruvathukal, 1967). These contours were developed from very few data points in the Portland Hills so the position of the contours could vary, which would effect the modeled position of the "sediment-volcanic interface". The fact that the interface locations on the Kings Heights-Albina Line (E-E') and the Oak Grove Line (G-G') are based on detailed data and coincide with the north-northwest trend defined by the other models increases the probable reliability. Data from the Barber well (BW) suggests that the well is located east of the change in slope of the "sediment-volcanic interface" (see Figure 3). This would necessitate changing the trend to northwesterly north of the Stark Street Line (B-B'). These uncertainties and variations illustrate that the trend and location of the "sediment-volcanic interface", shown on Figure 18, is approximate.

Intrusion

On Figure 18, a heavy line encircles the modeled extent of the intrusion. The interior contours are 0.5 km isopachs illustrating the thickness of the intrusion. Only models using an intrusion density of 3.0 gm/cm^3 were used as data sources. This outline corresponds very closely with the gravity high.

The contours shown in Figure 18 violate two data points. The Sellwood Line (F-F') model does not extend the intrusion as far to the east or west as in other models. The detailed portion of this line is about 3 km long and ends between the north- and northwest-trending lobes of the gravity high on the east, as shown on Plate 2. Extending the line from the Complete Bouguer Gravity Anomaly Map of Oregon (Berg and Thiruvathukal, 1967) would show no increase in gravity values, as shown in Figure 16, and consequently, no intrusion was necessary east of the east end of the line. If the data on Plate 2 had been available at the time of modeling, it appears that the intrusion would extend farther east than shown on Figure 16. Similar circumstances occur on the west end of the line.

A discrepancy also exists between the thickness of the intrusion in the Oak Grove Line and the Clackamas Highway Line models. The Oak Grove Line intrusion is approximately 400 m thinner east of the Portland Hills Fault and 1000 m thinner west of the Portland Hills Fault. The majority of the discrepancy is due to a different interpretation on the amount of offset on the Portland Hills Fault. Jones interprets 300 m of offset on the Portland Hills Fault which juxtaposes about 200 m of channel fill, having a density of 2.2 gm/cm^3 against the intrusion, having a density of 3.0 gm/cm^3 . The author interprets

only 120 m of offset on the Portland Hills Fault and accounts for the remainder of the gravity difference by thickening the intrusion which juxtaposes 800 m of Skamania Volcanics, density 2.8 gm/cm^3 against the intrusion. Values for the Clackamas Highway Line are used in Figure 18.

Despite these discrepancies, this composite view of the intrusion illustrates the general shape of the proposed feature. The east-west lateral extent remains quite constant throughout the study area at about 14 km. The northern boundary forms a blunt nose along the Columbia Boulevard Line (A-A'). The southern boundary lies south of the study area. The Complete Bouguer Gravity Anomaly Map of Oregon (Berg and Thiruvathukal, 1967) shows the gravity high centered about 15 km south of the study area in the vicinity of Highland Butte.

The modeled intrusion is shaped like a sill with the thickness to width ratio increasing from 0.04 at the Stark Street Line (B-B') to 0.10 along the Clackamas Highway Line (D-D'). Another characteristic of the intrusion shown in all models is the abrupt western edge as opposed to the gradual thinning on the eastern edge. The abruptness of the western edge may indicate structural control.

Mt. Scott

A different method of modeling was attempted over Mt. Scott, a Boring Lava vent. Gravity values were measured across the vent where good elevation control was available. The gravitational effect of Mt. Scott was calculated using various densities. The results of these calculations, with the regional gradient removed, are shown with the topography across the vent in Figure 19. Since no one density produces a flat line in Figure 19, the density of the material probably varies across the vent. The top of Mt. Scott appears to have the lowest density, while the flanks are denser. The lower densities near the vent may represent brecciation or an abundance of cindery material. More data across other Boring Lava vents is needed to determine if this is a common characteristic of other Boring Lava vents. In many vent areas, Allen (1975) found resistant plugs of massive lava surrounded by outward dipping layers of cinders, which would produce the opposite density profile of that shown on Figure 19.

GEOLOGIC IMPLICATIONS OF THE GRAVITY MODELS

The gravity models from this study and previous studies and their compilation in Figure 18 suggest many questions about the geologic history of the Portland area. Although these models can not resolve these questions,

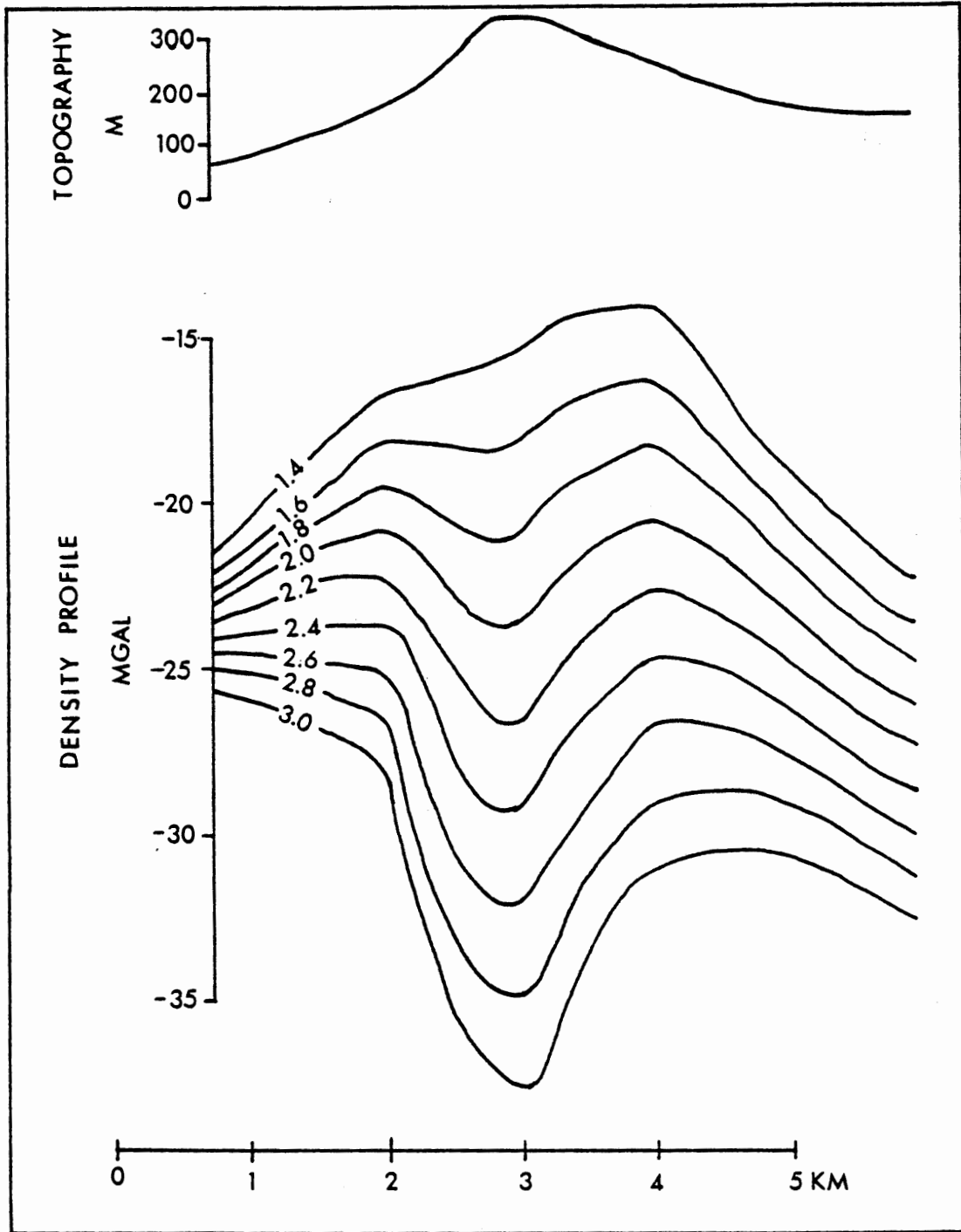


Figure 19. Mt. Scott topography and density profile. Densities in gm/cm^3 .

they do provide some alternative possibilities and illustrate some limiting factors under which the various alternatives must be explained. Questions concerning structures in the Columbia River basalt, the origin and development of the "sediment-volcanic interface", the relationship of the intrusion to the surrounding rock types, and movements on the Portland Hills Fault are discussed in the following section.

Structures in the Columbia River basalt

Few significant structures in the Columbia River basalt beneath the Portland Basin were identified in this study. The offsets identified and shown on Figure 18 form a general pattern of a graben beneath the Portland Basin, trending north-northwest. Allen (1975) points out that many volcanic fields around the world are formed in grabens and suggests that the Boring volcanoes might be related to this type of deformation.

Since the Boring Lava was erupted through the Columbia River basalt, Beeson and others (1976) and Allen (1975) hypothesized that vent locations might be controlled by fractures or faults in the Columbia River basalt. One of the most prominent vent alignments suggested by Allen was along the Yamhill-Bonneville Lineament discussed in Hammond (1971) and located on Figure 2. Hammond described the structure as a wide

zone of east-northeast-trending en echelon faults having a maximum left-lateral separation across the zone of 40 km (25 miles) in as little as the past 8 million years. In the study area, the lineament is described as a broad rectilinear fracture zone which might have allowed the upward migration of Boring Lava at fracture intersections. These trends are not reflected in the gravity values, however such a fracture system need not have appreciable vertical offsets, which are necessary for detection by gravity methods.

If considerable left-lateral movement on the lineament has occurred, offsets of the Portland Hills Fault, the intrusion, and the "sediment-volcanic interface" should be reflected in the gravity data. The observed gravity values do not indicate these displacements.

Eocene to Oligocene "Sediment-Volcanic Interface"

The geometry of the Eocene to Oligocene "sediment-volcanic interface" has been interpreted in various ways in the past. Beeson and others (1976) represented the Skamania Volcanics in schematic illustrations as a ridge of volcanics, interfingering on either side with adjacent sediments. Jones (1977) interpreted the feature in a like manner as he proposed that the intrusion assimilated the material in a sedimentary basin, adjacent to and east of the volcanics. If the modeled intrusions did not

assimilate sedimentary material, the gravity models portray the Skamania Volcanics with a steep western slope and a broad, flat top extending through the study area. The outcrop pattern in Washington, shown in Figure 2, also suggests a broad feature.

The alignment of the hatchured zones in Figure 18 suggests that the change in slope of the "sediment-volcanic interface" may be structurally controlled. Beck and Burr (1979) proposed that the Skamania Volcanics may represent the initial stages of a volcanic arc, which are characteristically linear. The volcanism might have been controlled by a remnant suture zone left when the subduction zone moved westward in Eocene time. If the "sediment-volcanic interface" is a linear feature, the occurrence on the Columbia Boulevard Line (A-A') requires tectonic displacement, which will be discussed later.

As an alternative, the linearity shown on Figure 18 may not be representative of the entire feature. Late Eocene through Oligocene time was dominated by localized volcanic centers, separated by basins (Snively and Wagner, 1963). The zone shown west of the Portland Hills Fault (PHF) in Figure 18 and the location on the Columbia Boulevard Line may reflect isolated volcanic centers rather than a continuous linear feature.

Intrusion

The gravity models in this study and previous studies have established a connection between the gravity high and the modeled intrusion. The Complete Bouguer Gravity Anomaly Map of Oregon (Berg and Thiruvathukal, 1967), Figure 5, shows that the gravity high continues to increase south of the study area and is centered near Highland Butte (HB on Figure 2). This area is a major Boring Lava center as shown on Figure 2, and consequently Beeson and others (1976) and Jones (1977) hypothesized that the intrusion was related to the Boring Lava occurrences. Beeson (1976) also relates the formation of graben structures in units as young as the Troutdale Formation in the Portland area to the withdrawal of Boring magma from near surface chambers and channels to the location of the modeled intrusion. This interpretation also suggests that the intrusion is related to the Boring Lavas.

The relationship between the modeled intrusion and Boring Lava occurrences is shown on Figure 20. The extent of the intrusion west of the Portland Hills Fault is unknown at this time, but it was not required in the Kings Heights-Albina Line (E-E') (Johnson and others, 1976). The distance of some of the vents from the intrusion does not preclude the possibility that the intrusion may be the source of the Boring Lava, because mafic magma should

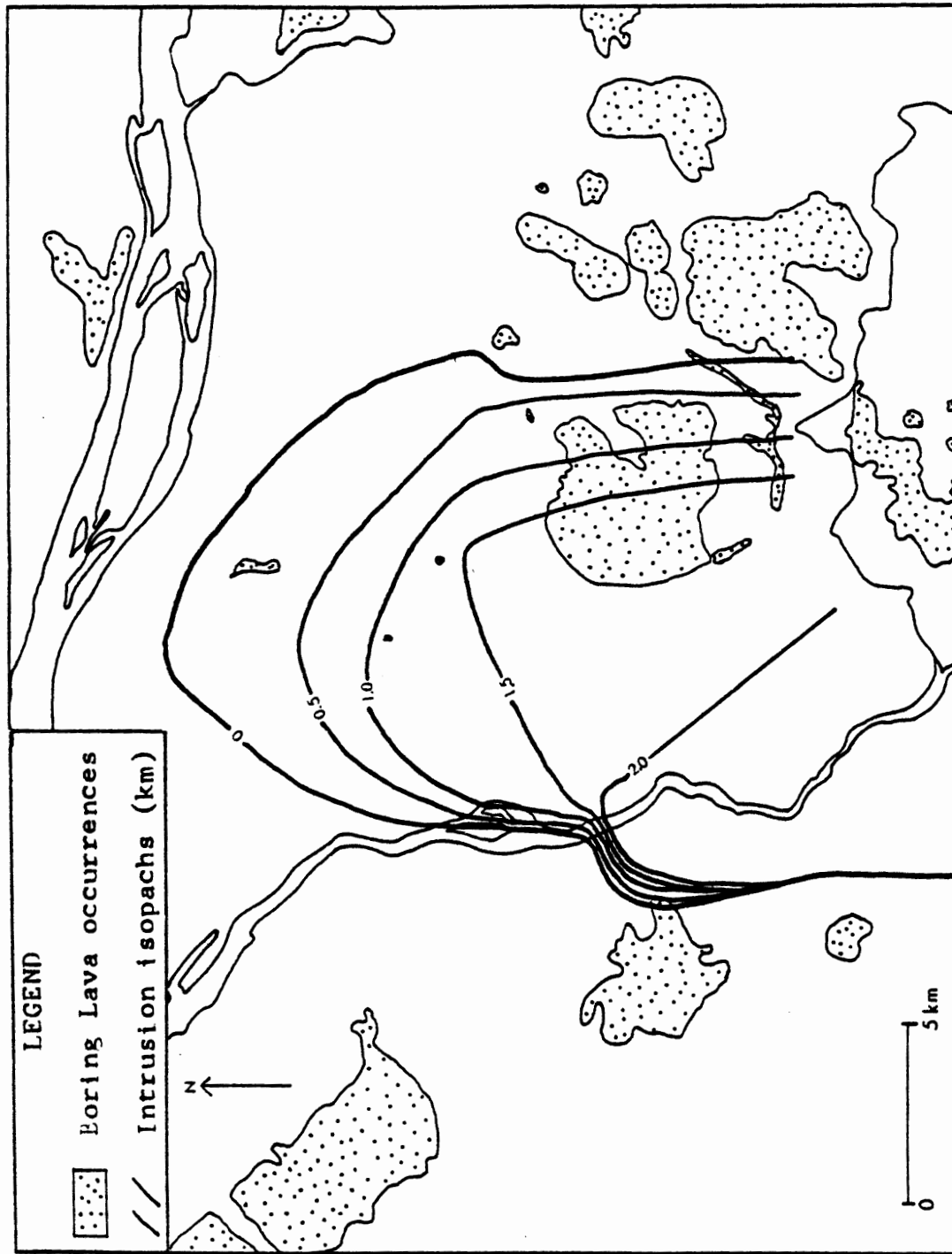


Figure 20. Spatial relationship between the modeled intrusion and Boring Lava occurrences.

be fluid enough to travel long distances through fractured or jointed rocks.

The abrupt western edge of the modeled intrusion suggests structural control. The intrusion may have followed a pre-existing structural weakness in the Skamania Volcanics. Jones (1977) hypothesized that the location of the intrusion was controlled by an ancient sedimentary basin adjacent to the Skamania Volcanics. He argues that the sediments would be more easily assimilated or displaced by the magma. This possibility does not explain the modeled abrupt west boundary of the intrusion, and it is doubtful that if assimilation had occurred, a density of 3.0 gm/cm^3 would still have been possible.

As an alternative hypothesis, the intrusion may have been part of the Skamania Volcanics. The dense material may represent a more slowly cooled core in the volcanic terrain. All models locate the intrusion within the Skamania Volcanics which supports this hypothesis. The sill-like geometry of the intrusion however does not correspond with the idealized shape of a volcanic core, which would be more dike-like or equidimensional. The proximal relationship between the Boring Lava and the intrusion could be explained by the intrusion of the Boring magma along the same structure or weakness

zone that controlled the intrusion. If the intrusion is older than the Boring Lavas, the Boring magma would be more likely to move around the periphery of the intrusion rather than through it. Both north and south of the study area, exposures of Boring Lava and Skamania Volcanics occur in very close proximity with one another.

These two hypotheses provide two options for the time of emplacement of the intrusion; either about 35 m.y.b.p. (Beck and Burr, 1979) or 1 to 10 m.y.b.p. (Trimble, 1963), associated with the Boring Lavas.

Movement on the Portland Hills Fault

Modeling by Johnson and others (1976) and Jones (1977) was consistent with vertical offsets, down to the east, along the Portland Hills Fault. The model for the only line which was surveyed in detail across the fault in this study (Clackamas Highway Line) is consistent with vertical faulting. Beeson and others (1976) also postulated right-lateral movement along this zone in order to produce the sub-parallel en echelon folds of the Portland Hills. This sense of movement is also consistent with focal mechanism solutions from earthquakes in northwestern Oregon (Cash, 1974). Right-lateral movement along the Portland Hills Fault is a possible explanation for some of the structural complications encountered during this study.

If the "sediment-volcanic interface" formed as a continuous linear feature, then its position along the Columbia Boulevard Line (A-A') must be due to tectonic displacement. Figure 21 schematically illustrates the situation if the displacement was the result of right-lateral movement along the Portland Hills Fault. If the trend of the "sediment-volcanic interface" is approximately N 10 W, as indicated in Figure 18, and the Portland Hills Fault trends approximately N 35 W, then the amount of right-lateral offset along the Portland Hills Fault necessary to bring the interface to the modeled position along the Columbia Boulevard Line would be about 22 km. The "sediment-volcanic interface" on the Columbia Boulevard Line is presumed to parallel the "sediment-volcanic interface" west of the Portland Hills Fault. If the trend of the interface increases to N 20 W, the amount of offset increases to approximately 50 km. In both cases, the movement would be post-Oligocene. Using the outcrop distribution of the Skamania Volcanics in Washington and Oregon, Beeson and others (1976) postulated right-lateral displacement along the Portland Hills Fault of up to 40 km. They also interpreted offsets in Bouguer anomaly contours suggesting approximately 30 km of right-lateral displacement.

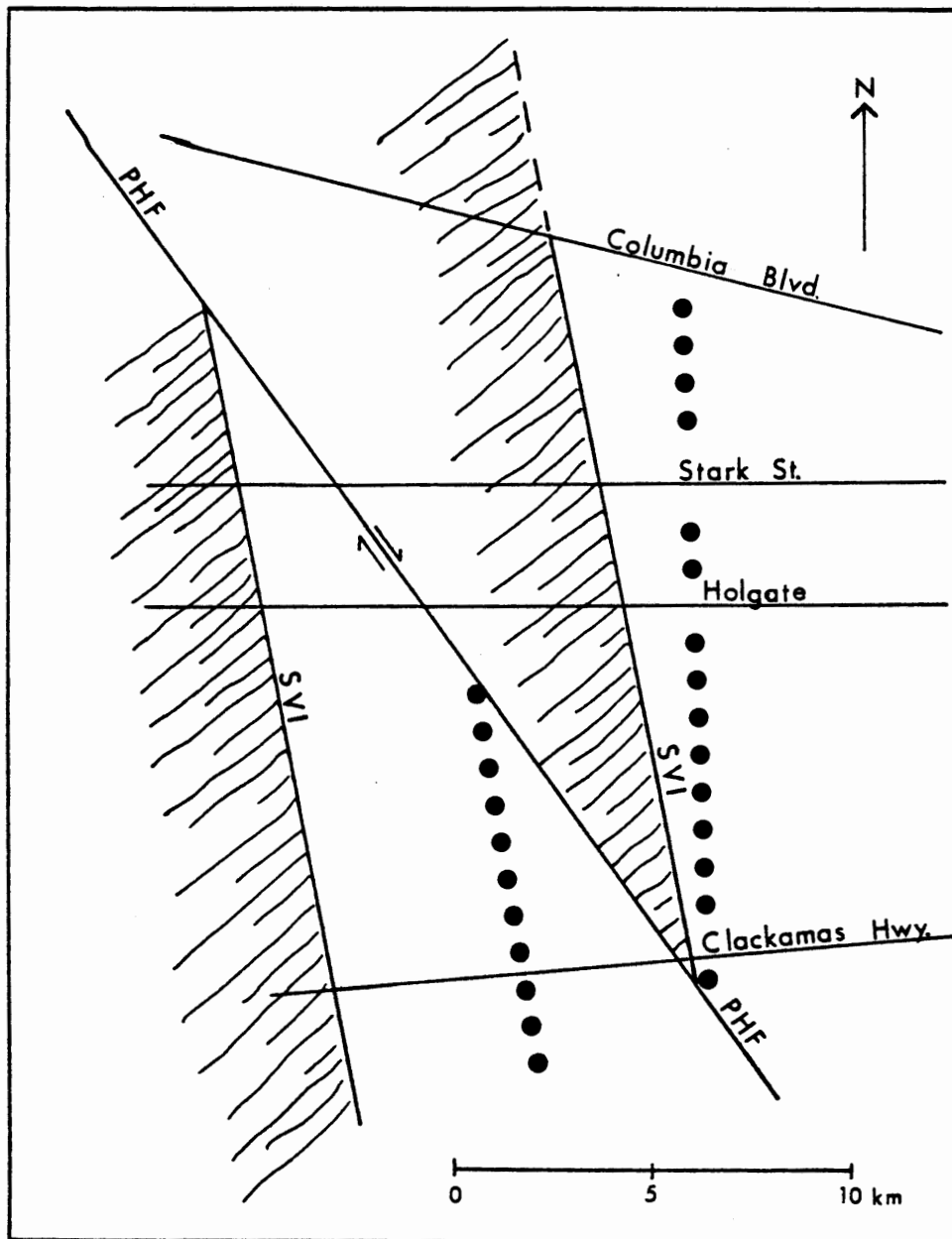


Figure 21. Schematic illustration of right-lateral offset on the Portland Hills Fault. Abbreviations: CI = center of intrusion; PHF = Portland Hills Fault; SVI = "sediment-volcanic interface".

If the "sediment-volcanic interface" is assumed to trend N 10 W, the intersection of the trend from the Columbia Boulevard Line and the Portland Hills Fault occurs at the intersection of the north-trending gravity high and the Portland Hills Fault on Plate 2. Since the gravity high reflects the intrusion, it is possible that the "sediment-volcanic interface" may have controlled the position of the intrusion.

The approximate locations of the gravity models developed for this study are also shown on Figure 21. The displacement of the "sediment-volcanic interface" along the Portland Hills Fault would juxtapose different parts of the volcanic terrain. For instance, the Stark Street Line should cross two changes in slope of the "sediment-volcanic interface". This is not reflected in the models (Figures 10 and 11) constructed for this line. The occurrence of the intrusion in this area might mask the increasing sediment thickness predicted by Figure 21. The sediment wedge between the eastern "sediment-volcanic interface" and the Portland Hills Fault would decrease in thickness southward. South of the Clackamas Highway Line, the thickness of volcanic rocks on either side of the fault would be the same.

Alternatively, the location of the "sediment-volcanic interface" on the Columbia Boulevard Line would be due to

different amounts of rotation between small crustal blocks or to right-lateral displacement along an east-west-trending fault between the Columbia Boulevard Line and the Stark Street Line. Also as discussed earlier, the "sediment-volcanic interface" may not be a continuous linear feature, in which case no displacement would be required.

Because other evidence in Beeson and others (1976) and Anderson (1978) supports right-lateral movement along the Portland Hills Fault, the author prefers this interpretation. Consequently, the Columbia Boulevard models shown in Figures 7 and 8 show a right-lateral fault along the Portland Hills Fault trend.

The strongest expression of the Portland Hills Fault on Plate 2 occurs in the southwest corner of the study area. The Clackamas Highway model, shown in Figure 14, proposed that the majority of the gravity increase across the fault was due to thickening the intrusion west of the fault to 2300 m in comparison to a thickness of 1500 m east of the fault. The juxtaposition of the different intrusive thicknesses could be due to right-lateral movement along the Portland Hills Fault. The line of dots in Figure 21 represents the approximate center locations of the intrusions. The amount of right-lateral separation on the Portland Hills Fault between the two segments is about 10 km. With the center of the intrusion located south of

the study area, the occurrence of the thinner sill east of the fault would be what one would expect, as it would have originally been located farther north.

If the intrusion is an integral part of the Skamania Volcanics, the displacement would have to occur within about the last 35 million years; a movement rate of 0.03 cm/yr. If the intrusion is related to the Boring Lavas, the movement would have to occur within the last 1 to 10 million years, requiring a rate of movement from 1 cm/yr to 0.1 cm/yr. No offsets along the Portland Hills Fault trend have been found in units younger than the Columbia River basalt. Rates of movements on the order of 0.1 cm/yr might be concealed by rapid weathering, but rates approaching 1 cm/yr should be apparent.

The variable thicknesses of the intrusion across the Portland Hills Fault can be explained without right-lateral movement on the fault after the emplacement of the intrusion. The Portland Hills Fault could act as a restraining boundary for the movement of the magma. It may have diverted much of the magma to the northwest-trending nose and allowed a lesser amount through to form the thinner north-trending nose. As another alternative, prior movement along the Portland Hills Fault might have juxtaposed host rocks having different transmissibilities which would affect the distribution of the magma.

Although the interpretation of the gravity models has not resulted in a definitive assessment of the amount of right-lateral movement which has occurred along the Portland Hills Fault, it has provided some guidelines. Reasonable amounts of movement in the last 35 million years range from 10 km to 50 km, while the amount of movement in the last 10 million years should be less than 10 km.

REGIONAL IMPLICATIONS

The geologic features shown in the models developed for this study do not require the reinterpretation of any regional structures. The northwest-trending syncline with associated vertical offsets in the Columbia River basalt beneath the Portland Basin, and the right-lateral, as well as vertical movement along the Portland Hills Fault are consistent with regional stress patterns. The existence of an intrusion, whether genetically associated with the Skamania Volcanics or the Boring Lava, is not unusual in an area of such extensive volcanism.

CONCLUSIONS

The gravity survey and structural interpretation of the Portland Basin completed for this study have resulted in a better definition of several proposed geologic features beneath the Columbia River basalt, but did not provide as much information on structures within the basalt as had been anticipated. The Complete Bouguer Gravity Anomaly Map of the Portland Basin, based on about 750 gravity stations, is consistent with the Complete Bouguer Gravity Anomaly Map of Oregon by Berg and Thiruvathukal (1967). The gravity map of the Portland Basin shows a strong decreasing gravity trend from west to east across the study area which is attributed to crustal thickening. Other features which are prominent are gravity highs, trending north and northwest, a sharp decreasing gradient from west to east across the trend of the Portland Hills Fault, and a gravity low in the northwest corner of the study area. Westward extensions of the gravity data from the Complete Bouguer Gravity Anomaly Map of Oregon show rapidly decreasing gravity west of the study area. There is no expression in the gravity values of the syncline in the Columbia River basalt defined by well log data.

Gravity modeling interpreted the gravity highs as a sill-shaped intrusion, having a density of 3.0 gm/cm^3 . The intrusion west of the Portland Hills Fault related to the northwest-trending gravity high is substantially thicker than the intrusion east of the Portland Hills Fault related to the north-trending gravity high. The extent of the intrusion west of the fault is unknown, while the intrusion east of the fault appears to extend nearly to the northern boundary of the study area. Increasing gravity south of the study area suggests that the intrusion is probably centered in that area. These intrusions may be related to the Boring Lavas or the Skamania Volcanic Series.

The sharp gravity gradient across the Portland Hills Fault trend in the southwest corner of the study area was interpreted as 120 m (400 ft) of offset in the Columbia River basalt, with the remainder of the anomaly accounted for by thickening of the intrusion west of the fault. Vertical offsets along the Portland Hills Fault trend are not included in other models developed for this study due to a lack of detailed data.

The decreasing gravity west of the study area was modeled as a westward sloping interface between Eocene sedimentary rocks and late Eocene to Oligocene sedimentary rocks and volcanic rocks of the Skamania Volcanic Series and the Siletz River Volcanic Series. The locations of

this feature, named the "sediment-volcanic interface" on the models formed a north-northwest trend roughly beneath the Portland Hills.

The gravity low in the northwest corner of the study area required a thickness of sediments east of the Portland Hills greater than predicted by projections of the available well log data.

Right-lateral movement along the Portland Hills Fault was proposed as a possible explanation for the increased sediment thickness in the northwest corner of the study area and for the varying intrusive thicknesses across the fault in the southwest corner of the study area.

Although the north-trending gravity high and associated intrusion tended to obscure shallower features, modeling the structure of the Columbia River basalt as a flat-bottomed syncline as indicated by the well log data was consistent with the gravity data. Minor faulting on the east and west limbs of the syncline, indicated by small wavelength changes in gravity values, produced a graben-like structure beneath the Portland Basin.

REFERENCES CITED

- Allen, J.R., 1975, Volcanoes of the Portland area, Oregon: Ore Bin, vol. 37, no. 9, p. 145-157.
- Anderson, J.L., 1978, The stratigraphy and structure of the Columbia River basalt in the Clackamas River drainage: Portland, Ore., Portland State University master's thesis, 136 p.
- Atwater, T.M., 1970, Implication of plate tectonics for the Cenozoic tectonic evolution of western North America: Geol. Soc. America Bull., v. 81, p. 3513-3536.
- Baldwin, E.M., 1975, Revision of the Eocene stratigraphy of southwestern Oregon, in Weaver, D.W., Hornday, G.R. and Tipton, A., eds., Paleogene Symposium and Selected Technical Papers: Annual Meeting, Pacific Sections, AAPG, SEPM, SEG, Long Beach, California, April 1975, p. 49-64.
- Baldwin, E.M., Brown, R.D., Gair, J.E. and Pease, M.H., Jr., 1955, Geology of the Sheridan and McMinnville quadrangles, Oregon: U.S. Geol. Survey Oil and Gas Inv. Map OM 155.
- Balsillie, J.H. and Benson, G.T., 1971, Evidence for the Portland Hills Fault: The Ore Bin, v. 33, no. 6, p. 109-118.
- Beaulieu, J.D., 1971, Geologic formations of western Oregon: Oregon Dept. Geol. and Mineral Industries Bulletin, 70, 72 p.
- Beck, M.E., Jr. and Burr, C.D., 1979, Paleomagnetism and tectonic significance of the Goble Volcanic Series, southwestern Washington: Geology, v. 7, p. 175-179.
- Beeson, H.M., Bentley, R.D., and Moran, M.R., 1976, Preliminary correlation of lower Yakima Basalt flows in western Oregon with the type area in central Washington (abs): 72nd Annual Meeting, Cordilleran Section, Geol. Society of America.

- Benson, G.T. and Donovan, J.C., 1974, Preliminary tectonic map of the Greater Portland area, in Hammond, P.E. and others, 1974, A Preliminary Geological Investigation of the Ground Effects of Earthquakes in the Portland Metropolitan Area, Oregon: unpublished report to the U.S. Geological Survey (PEG I report).
- Berg, J.W., Jr. and Thiruvathukal, J.V., 1967, Complete Bouguer Gravity Anomaly Map of Oregon, Oregon Department of Geology and Mineral Industries, Geological Map Series, GMS 4-b.
- Bonini, W.E., Hughes, D.W., and Danes, Z.F., 1974, Complete Bouguer Gravity Anomaly Map of Washington, Division of Geology and Earth Resources, State of Washington, Department of Natural Resources, Geologic Map GM-11.
- Bromery, R.W., and Snavely, P.D., Jr., 1964, Geological interpretation of reconnaissance gravity and aeromagnetic surveys in northwest Oregon: U.S. Geol. Survey Bull., 1181-N.
- Burch, D, in progress, An analysis and correlation of the Boring Lavas using geochemical, petrographic and paleomagnetic data: Portland State Univ., M.S. thesis.
- Cash, 1973, A gravity survey in N.E. Portland, unpublished.
- Cash, D.J., 1974, Portland earthquake history, in Hammond, et al, 1974, A Preliminary Geological Investigation of the Ground Effects of Earthquakes in the Portland Metropolitan Area, Oregon, unpublished report to U.S. Geol. Survey.
- Diller, J.S., 1896, A geological reconnaissance in northwestern Oregon: U.S. Geol. Survey 17th Ann. Rept. Pt. 1, p. 441-520.
- Diller, J.S., 1898, Description of the Roseburg quadrangle: U.S. Geol. Survey Atlas, Folio 49.
- Dobrin, M.B., 1976, Introduction to Geophysical Prospecting: New York: McGraw-Hill Book Co., Inc., 630 p.

- Felts, W.M., 1939a, A granodiorite stock in the Cascade Mountains of southwestern Washington: *Ohio Jour. Sci.*, v. 39, no. 6, p. 297-316.
- Felts, W.M., 1939b, Keechelus andesitic lava flows of Washington in southward extension: *Pan-Am. Geologist*, v. 71, no. 4, p. 294-296.
- Griffin, W.C., Watkins, F.A., Jr. and Swenson, H.A., 1956, Water resources of the Portland, Oregon, and Vancouver, Washington, area: *U.S. Geol. Survey Circ.*, 372.
- Hammond, P.E., 1971, Plate tectonics and the Yamhill-Bonneville structure zone in northwestern Oregon (abs): *The Geological Newsletter, Geological Society of the Oregon Country*, v. 38, no. 3, p. 3-5.
- Hammond, P.E., Benson, G.T., Cash, D.J., Palmer, L.A., Donovan, J.C. and Gannon, B., 1974, A Preliminary Geologic Investigation of the Ground Effects of Earthquakes in the Portland Metropolitan Area, Oregon, unpublished report to the U.S. Geological Survey, 40 p.
- Hodge, E.T., 1933, Age of the Columbia River and lower canyon (Abst.): *Pan American Geol.*, v. 58; No. 1, p. 70, Aug. 1932; (abst.) *Geol. Soc. America Bull.*, v. 44, p. 156, 1933.
- Hogenson, G.M. and Foxworthy, B.L., 1965, Ground Water in the East Portland Area, Oregon: *U.S. Geol. Survey Water-supply Paper* 1793.
- Hunting, M.T., Bennett, W.A.G., Livingston, V.E., Jr., and Moen, W.S., 1961, Geologic map of Washington: *Wash. Div. Mines and Geology*.
- Johnson, A.G., 1975, Gravity profiles across the northeast side of the Tualatin Mountains, Portland, Oregon (abs.): *Transactions, American Geophysical Union*, December, 1975, p. 89.
- Johnson, A.G., Donovan, J.C. and Moran M.R., 1976, Gravity surveys across the northeast side of the Portland Hills, Oregon, in Beeson and others, 1976, *Portland Environmental Geology - Fault Identification*, unpublished report to the U.S. Geological Survey, p. 36-64.

- Jones, T.D., 1977, Analysis of a gravity traverse south of Portland, Oregon: Portland State Univ., B.S. thesis, 54 pg.
- Maxwell, J.C., 1974, Early western margin of the United States, in Burk, C.A. and Drake, C.L., eds., The Geology of Continental Margins, p. 831-852.
- Nettleton, L.L., 1971, Elementary Gravity and Magnetics for Geologists and Seismologists, Society of Exploration Geophysicists Monograph, Series No. 1, 121 p.
- Newton, V.C., Jr., 1969, Subsurface Geology of the Lower Columbia and Willamette Basins, Oregon: Oregon Department of Geology and Mineral Industries, Oil and Gas Investigation, No. 2, 121 p.
- Perttu, R.K., 1976, Structural geology of the northeast quarter of the Dutchman Butte quadrangle, Oregon: Portland State Univ. master's thesis, 60 p., unpublished.
- Perttu, R.K. and Benson, G.T., 1980, Deposition and deformation of the Eocene Umpqua Group, Sutherlin area, southwestern Oregon: Oregon Geology, v. 42, no. 8, p. 135-140.
- Piper, A.M., 1942, Ground-water resources of the Willamette Valley: U.S. Geol. Survey WSP 890.
- Russel, J.C., 1893, A geological reconnaissance in central Washington: U.S. Geol. Survey Bull. 108, p. 20-22, map.
- Schenck, H.G., 1927, Marine Oligocene of Oregon: Calif. Univ. Publ. Geol. Sci., v. 16, no. 12, p. 449-460.
- Schmela, R.J., 1971, Geophysical and geological analysis of a fault-like linearity in the Lower Clackamas River Area, Clackamas County, Oregon: Portland State Univ. M.S. thesis, 113 p.
- Simpson, R.W. and Cox, A.V., 1977, Paleomagnetic evidence for tectonic rotation of the Oregon Coast Range: Geology, v. 5, p. 585-589.

- Snavely, P.D., Jr., and Baldwin, E.M., 1948, Siletz River Volcanic Series of northwestern Oregon: Am. Assn. Petroleum Geologists Bull., v. 32, no. 5, p.806-812.
- Snavely, P.D., Jr., MacLeod, N.S., and Wagner, H.C., 1968, Tholeiitic and alkalic basalts of the Eocene Siletz River Volcanics, Oregon Coast Range: American Journal of Science, v. 266, p. 454-481.
- Snavely, P.D., and Vokes, H.E., 1949, Geology of the coastal area between Cape Kiwanda and Cape Foulweather, Oregon: U.S. Geol. Survey Oil and Gas Inv. Map OM 97.
- Snavely, P.D., Jr. and Wagner, H.C., 1963, Tertiary geologic history of western Oregon and Washington: Wash. Div. Mines and Geol., R.I. 22.
- Snavely, P.D., Jr. and Wagner, H.C., 1964, Geologic sketch of northwestern Oregon: U.S. Geol. Survey Bull., 1181-M.
- Talwani, M., Worzel, J.C. and Landisman, M., 1959, Rapid gravity computations for two-dimensional bodies with application to the Mendocino submarine fracture zone: Jour. Geophys. Res., v. 64, no. 1, p. 49-59.
- Thiruvathukal, J.V., Berg, J.W., Jr., and Henricks, D.F., 1970, Regional gravity of Oregon: Geol. Soc. America Bull., v. 81, no. 3, p. 725-738.
- Treasher, R.C., 1942, Geologic history of the Portland area: Oregon Dept. Geol. and Mineral Industries Short Paper 7, 10 p., geol. map.
- Trimble, D.E., 1963, Geology of Portland, Oregon and adjacent areas: U.S. Geol. Survey Bull. 1119, map. Scale 1:62, 500.
- Turner, F.E., 1938, Stratigraphy and mollusca of the Eocene of western Oregon: Geol. Soc. America Spec. Paper 10, 130 p.
- Warren, W.C. and Norbistrath, Hans, 1946, Stratigraphy of the upper Nehalem River basin: American Assn. Petroleum Geologists Bull., v. 30, no. 2, p. 213-237.

Warren, W.C., Norbistrath, Hans, and Grivetti, R.M.,
1945, Geology of northwestern Oregon west of
the Willamette River and north of Lat. 45°15':
U.S. Geol. Survey Map OM-42.

Weaver, C.E., 1912, Preliminary report on the Tertiary
paleontology of western Washington: Washington
Geological Survey Bulletin, v. 15, 80 p.

Wells, F.G. and Peck, D.L., 1961, Geologic map of
Oregon west of the 121st meridian: U.S. Geol.
Survey Misc. Geol. Inv. Map 1-325.

APPENDIX

TABLE II

GRAVITY DATA

Latitude	Longitude	Elev. meters	T.C.* mgals	Observed Gravity mgals	Theoretical Gravity mgals	F.A.* Anomaly mgals	C.B.* Anomaly mgals
45° 36.15'	122° 40.25'	7.05	0.05	980641.70	980683.71	-39.83	-40.57
45° 36.06'	122° 39.25'	10.43	0.09	980643.90	980683.57	-36.45	-37.53
45° 36.04'	122° 39.75'	7.53	0.05	980642.80	980683.54	-38.42	-39.21
45° 36.02'	122° 38.56'	10.53	0.09	980645.70	980683.51	-34.56	-35.65
45° 36.02'	122° 38.05'	11.50	0.10	980646.10	980683.51	-33.86	-35.05
45° 36.02'	122° 37.25'	11.95	0.10	980646.00	980683.51	-33.82	-35.05
45° 35.74'	122° 44.58'	28.76	0.23	980631.70	980683.09	-42.51	-45.50
45° 35.74'	122° 35.45'	12.45	0.11	980646.60	980683.09	-32.65	-33.93
45° 35.64'	122° 43.06'	11.48	0.16	980637.30	980682.94	-42.09	-43.21
45° 35.64'	122° 43.06'	12.53	0.16	980636.90	980682.94	-42.17	-43.41
45° 35.64'	122° 43.06'	11.78	0.16	980636.90	980682.94	-42.40	-43.56
45° 35.64'	122° 43.06'	9.48	0.16	980637.60	980682.94	-42.41	-43.31
45° 35.57'	122° 45.39'	39.46	0.32	980629.20	980682.83	-41.46	-45.54
45° 35.57'	122° 43.89'	29.29	0.19	980632.30	980682.83	-41.49	-44.57
45° 35.33'	122° 41.77'	12.70	0.13	980638.10	980682.47	-40.45	-41.74
45° 35.14'	122° 41.16'	13.13	0.12	980638.50	980682.19	-39.63	-40.98
45° 35.10'	122° 44.80'	46.13	0.31	980628.60	980682.13	-39.29	-44.13
45° 35.00'	122° 34.61'	6.09	0.05	980646.94	980682.05	-33.22	-33.86
45° 34.98'	122° 40.00'	12.90	0.12	980640.30	980681.95	-37.67	-38.99
45° 34.80'	122° 44.17'	46.50	0.30	980628.80	980681.68	-38.52	-43.42
45° 34.74'	122° 39.14'	15.24	0.11	980642.60	980681.59	-34.28	-35.87
45° 34.65'	122° 34.61'	6.09	0.07	980645.54	980681.45	-34.03	-34.65
45° 34.63'	122° 40.05'	30.47	0.10	980637.00	980681.42	-35.02	-38.32
45° 34.60'	122° 43.75'	47.40	0.30	980629.70	980681.38	-37.05	-42.05

*T.C.= Terrain Correction, F.A. = Free Air, C.B. = Complete Bouguer.

TABLE II (Cont.)

Latitude	Longitude	Elev. meters	T.C. mgals	Observed Gravity mgals	Theoretical Gravity mgals	F.A. Anomaly mgals	C.B. Anomaly mgals
45° 34.52'	122° 38.20'	19.63	0.11	980643.00	980681.25	-32.19	-34.28
45° 34.49'	122° 42.39'	48.34	0.64	980631.50	980681.21	-34.79	-39.55
45° 34.43'	122° 34.58'	6.09	0.08	980645.43	980681.12	-33.81	-34.41
45° 34.42'	122° 43.19'	49.52	0.64	980630.40	980681.10	-35.42	-40.32
45° 34.42'	122° 37.73'	34.38	0.11	980640.40	980681.10	-30.09	-33.83
45° 34.39'	122° 34.58'	6.09	0.09	980645.84	980681.06	-33.34	-33.93
45° 34.21'	122° 36.47'	16.78	0.10	980645.50	980680.79	-30.11	-31.88
45° 34.19'	122° 41.91'	55.65	0.68	980630.80	980680.76	-32.78	-38.33
45° 34.19'	122° 39.80'	52.49	0.08	980632.80	980680.76	-31.76	-37.54
45° 34.09'	122° 35.64'	21.71	0.10	980644.10	980680.61	-29.81	-32.13
45° 34.04'	122° 37.16'	35.84	0.06	980640.40	980680.53	-29.07	-33.02
45° 34.00'	122° 35.23'	19.99	0.10	980643.80	980680.47	-30.50	-32.64
45° 33.88'	122° 34.75'	18.28	0.10	980643.74	980680.29	-30.91	-32.86
45° 33.88'	122° 34.58'	17.93	0.10	980643.00	980680.29	-31.76	-33.67
45° 33.77'	122° 37.16'	45.69	0.07	980638.10	980680.13	-27.92	-32.96
45° 33.77'	122° 34.31'	19.23	0.10	980642.10	980680.13	-32.09	-34.14
45° 33.74'	122° 41.78'	59.90	0.72	980631.30	980680.08	-30.29	-36.27
45° 33.74'	122° 41.19'	59.88	0.33	980631.40	980680.08	-30.20	-36.57
45° 33.74'	122° 40.56'	62.18	0.18	980630.90	980680.08	-29.99	-36.76
45° 33.74'	122° 39.89'	61.17	0.72	980631.40	980680.08	-29.80	-36.57
45° 33.73'	122° 34.62'	24.68	0.95	980641.66	980680.07	-30.79	-33.45
45° 33.57'	122° 33.58'	23.18	0.10	980639.90	980679.83	-32.77	-35.26
45° 33.50'	122° 42.16'	10.21	0.20	980641.90	980679.72	-34.67	-35.61
45° 33.50'	122° 37.16'	58.11	0.08	980635.20	980679.72	-26.59	-33.01
45° 33.50'	122° 32.77'	17.71	0.11	980639.50	980679.72	-34.75	-36.62
45° 33.46'	122° 34.62'	39.92	0.09	980638.63	980679.66	-28.71	-33.08
45° 33.37'	122° 39.88'	59.89	0.06	980632.80	980679.53	-28.24	-34.87
45° 33.35'	122° 31.63'	13.38	0.12	980637.90	980679.49	-37.46	-38.84
45° 33.23'	122° 37.16'	70.94	0.09	980631.90	980679.31	-25.52	-33.36
45° 33.21'	122° 34.69'	48.76	0.09	980636.48	980679.28	-27.75	-33.12
45° 33.17'	122° 30.59'	12.82	0.13	980637.50	980679.22	-37.77	-39.07

TABLE II (Cont.)

Latitude	Longitude	Elev. meters	T.C. mgals	Observed Gravity mgals	Theoretical Gravity mgals	F.A. Anomaly mgals	C.B. Anomaly mgals
45° 33.04'	122° 34.70'	67.36	0.08	980632.45	980679.03	-25.79	-33.24
45° 33.00'	122° 37.16'	76.12	0.10	980630.90	980678.97	-24.58	-32.98
45° 32.98'	122° 29.69'	16.91	0.13	980635.30	980678.94	-38.42	-40.18
45° 32.96'	122° 29.68'	16.71	0.13	980635.24	980678.91	-38.51	-40.25
45° 32.91'	122° 37.31'	75.44	0.11	980630.90	980678.83	-24.65	-32.98
45° 32.91'	122° 36.83'	76.72	0.08	980630.90	980678.83	-24.26	-32.75
45° 32.90'	122° 39.58'	54.33	0.06	980635.10	980678.82	-26.95	-32.96
45° 32.90'	122° 38.95'	47.01	0.07	980636.70	980678.82	-27.61	-32.79
45° 32.90'	122° 38.13'	52.62	0.09	980635.60	980678.82	-26.98	-32.77
45° 32.90'	122° 37.61'	75.13	0.11	980630.50	980678.82	-25.13	-33.42
45° 32.90'	122° 36.20'	77.42	0.06	980630.90	980678.82	-24.03	-32.62
45° 32.90'	122° 35.59'	77.76	0.06	980631.00	980678.82	-23.82	-32.45
45° 32.90'	122° 35.02'	75.45	0.07	980631.10	980678.82	-24.43	-32.80
45° 32.90'	122° 34.23'	72.49	0.19	980630.70	980678.82	-25.75	-33.66
45° 32.90'	122° 33.39'	63.09	0.19	980630.80	980678.82	-28.55	-35.40
45° 32.82'	122° 34.70'	73.76	0.07	980631.25	980678.70	-24.69	-32.86
45° 32.78'	122° 28.58'	26.66	0.15	980631.50	980678.64	-38.91	-41.74
45° 32.63'	122° 37.31'	52.23	0.12	980636.10	980678.41	-26.19	-31.91
45° 32.57'	122° 34.64'	73.76	0.06	980630.72	980678.32	-24.84	-33.02
45° 32.56'	122° 33.39'	84.09	0.12	980625.90	980678.31	-26.46	-35.74
45° 32.52'	122° 39.63'	53.42	0.07	980636.10	980678.25	-25.66	-31.57
45° 32.36'	122° 37.31'	51.67	0.10	980636.50	980678.01	-25.56	-31.24
45° 32.34'	122° 34.64'	61.56	0.05	980634.18	980677.98	-24.79	-31.63
45° 32.23'	122° 35.59'	66.65	0.03	980633.26	980677.81	-23.98	-31.40
45° 32.21'	122° 33.41'	84.14	0.08	980626.20	980677.78	-25.61	-34.94
45° 32.18'	122° 39.63'	42.21	0.08	980638.80	980677.73	-25.91	-30.55
45° 32.09'	122° 34.65'	68.58	0.04	980632.14	980677.60	-24.30	-31.92
45° 32.08'	122° 28.56'	60.69	0.10	980622.80	980677.58	-36.05	-42.74
45° 32.06'	122° 29.68'	66.64	0.06	980623.74	980677.55	-33.25	-40.64
45° 32.05'	122° 37.31'	55.66	0.08	980637.50	980677.54	-22.86	-29.00
45° 31.89'	122° 28.58'	70.35	0.09	980620.40	980677.30	-35.19	-42.96

TABLE II (Cont.)

Latitude	Longitude	Elev. meters	T.C. mgals	Observed Gravity mgals	Theoretical Gravity mgals	F.A. Anomaly mgals	C.B. Anomaly mgals
45° 31.88'	122° 39.63'	38.28	0.09	980640.70	980677.28	-24.77	-28.95
45° 31.82'	122° 37.31'	55.44	0.07	980636.50	980677.19	-23.58	-29.71
45° 31.82'	122° 35.53'	78.87	0.07	980629.01	980677.19	-23.84	-32.59
45° 31.81'	122° 33.41'	89.49	0.05	980625.10	980677.18	-24.46	-34.41
45° 31.81'	122° 29.68'	89.05	0.05	980618.13	980677.18	-31.56	-41.46
45° 31.80'	122° 34.72'	76.50	0.04	980630.08	980677.16	-23.47	-31.99
45° 31.59'	122° 35.53'	77.13	0.10	980631.11	980676.85	-21.93	-30.45
45° 31.59'	122° 33.41'	88.26	0.04	980625.30	980676.85	-24.31	-34.13
45° 31.59'	122° 28.55'	75.80	0.07	980618.70	980676.85	-34.75	-43.15
45° 31.58'	122° 34.73'	76.19	0.03	980629.98	980676.83	-23.34	-31.82
45° 31.58'	122° 29.70'	89.81	0.05	980617.45	980676.83	-31.67	-41.66
45° 31.45'	122° 35.89'	73.79	0.12	980632.60	980676.64	-21.26	-29.40
45° 31.42'	122° 37.31'	50.26	0.06	980637.90	980676.59	-23.18	-28.74
45° 31.39'	122° 36.45'	62.75	0.09	980634.90	980676.55	-22.28	-29.21
45° 31.39'	122° 36.06'	69.22	0.11	980633.60	980676.55	-21.58	-29.22
45° 31.39'	122° 35.27'	78.28	0.12	980633.90	980676.55	-18.49	-27.12
45° 31.39'	122° 34.48'	84.78	0.04	980627.50	980676.55	-22.88	-32.32
45° 31.39'	122° 33.44'	85.95	0.03	980625.60	980676.55	-24.42	-34.00
45° 31.37'	122° 38.53'	42.98	0.10	980640.00	980676.52	-23.25	-27.96
45° 31.37'	122° 37.83'	58.44	0.07	980636.10	980676.52	-22.38	-28.84
45° 31.37'	122° 32.72'	87.76	0.03	980623.80	980676.52	-25.63	-35.41
45° 31.37'	122° 32.17'	72.84	0.03	980622.40	980676.52	-31.64	-39.75
45° 31.37'	122° 31.25'	94.55	0.03	980618.30	980676.52	-29.04	-39.58
45° 31.36'	122° 34.61'	77.72	0.04	980629.89	980676.50	-22.63	-31.28
45° 31.35'	122° 30.64'	93.49	0.04	980617.60	980676.49	-30.03	-40.45
45° 31.34'	122° 35.60'	111.75	0.39	980624.42	980676.47	-17.56	-29.67
45° 31.34'	122° 29.72'	81.26	0.05	980619.10	980676.47	-32.29	-41.33
45° 31.33'	122° 28.86'	76.89	0.06	980618.70	980676.46	-34.03	-42.56
45° 31.32'	122° 28.56'	76.22	0.06	980618.40	980676.44	-34.52	-42.98
45° 31.29'	122° 39.63'	14.55	0.17	980645.90	980676.40	-26.00	-27.46
45° 31.22'	122° 37.61'	50.80	0.05	980637.85	980676.30	-22.77	-28.40

TABLE II (Cont.)

Latitude	Longitude	Elev. meters	T. C. mgals	Observed Gravity mgals	Theoretical Gravity mgals	F. A. Anomaly mgals	C. B. Anomaly mgals
45° 31.21'	122° 38.66'	34.50	0.09	980641.93	980676.28	-23.70	-27.47
45° 31.18'	122° 38.40'	45.16	0.07	980639.88	980676.23	-22.41	-27.38
45° 31.17'	122° 39.76'	8.90	0.19	980646.37	980676.22	-27.10	-27.90
45° 31.17'	122° 39.26'	20.00	0.13	980644.68	980676.22	-25.36	-27.47
45° 31.17'	122° 39.02'	25.91	0.11	980643.70	980676.22	-24.52	-27.31
45° 31.17'	122° 38.02'	42.20	0.06	980640.47	980676.22	-22.72	-27.38
45° 31.17'	122° 37.77'	47.23	0.06	980639.06	980676.22	-22.58	-27.80
45° 31.16'	122° 37.31'	53.97	0.05	980637.39	980676.21	-22.16	-28.14
45° 31.16'	122° 37.13'	54.99	0.05	980637.21	980676.21	-22.03	-28.12
45° 31.16'	122° 36.97'	55.92	0.05	980637.08	980676.21	-21.87	-28.07
45° 31.16'	122° 36.67'	59.57	0.07	980635.98	980676.21	-21.85	-28.44
45° 31.16'	122° 36.18'	75.15	0.13	980632.77	980676.21	-20.24	-28.51
45° 31.16'	122° 35.93'	95.62	0.25	980628.79	980676.21	-17.91	-28.35
45° 31.16'	122° 35.52'	142.89	0.70	980617.71	980676.20	-14.39	-29.66
45° 31.16'	122° 31.84'	90.83	0.03	980621.57	980676.20	-26.60	-36.72
45° 31.16'	122° 31.50'	92.65	0.03	980619.79	980676.20	-27.18	-38.14
45° 31.16'	122° 31.13'	90.52	0.03	980619.19	980676.20	-29.07	-39.16
45° 31.16'	122° 30.80'	90.52	0.03	980618.74	980676.20	-29.52	-39.61
45° 31.16'	122° 30.52'	87.78	0.03	980619.28	980676.20	-29.83	-39.61
45° 31.16'	122° 30.14'	81.99	0.03	980619.75	980676.20	-31.15	-40.28
45° 31.16'	122° 29.81'	78.63	0.04	980619.88	980676.20	-32.05	-40.81
45° 31.16'	122° 29.52'	77.41	0.04	980619.52	980676.20	-32.79	-41.40
45° 31.16'	122° 29.20'	76.19	0.05	980619.26	980676.20	-33.42	-41.90
45° 31.16'	122° 28.89'	75.59	0.05	980618.92	980676.20	-33.95	-42.35
45° 31.16'	122° 28.55'	75.59	0.06	980619.27	980676.20	-33.60	-42.00
45° 31.16'	122° 28.25'	75.28	0.06	980618.71	980676.20	-34.26	-42.61
45° 31.16'	122° 27.91'	75.89	0.07	980618.58	980676.20	-34.20	-42.61
45° 31.16'	122° 27.55'	75.59	0.08	980618.07	980676.20	-34.80	-43.17
45° 31.16'	122° 27.23'	74.98	0.08	980617.99	980676.20	-35.07	-43.37
45° 31.16'	122° 26.89'	73.15	0.09	980617.97	980676.20	-35.65	-43.74
45° 31.16'	122° 26.55'	80.77	0.10	980616.34	980676.20	-34.93	-43.86

TABLE II (Cont.)

Latitude	Longitude	Elev. meters	T. C. mgals	Observed Gravity mgals	Theoretical Gravity mgals	F. A. Anomaly mgals	C. B. Anomaly mgals
45° 31.16'	122° 26.27'	90.52	0.11	980614.46	980676.20	-33.80	-43.81
45° 31.16'	122° 25.95'	99.97	0.13	980612.40	980676.20	-32.95	-43.99
45° 31.16'	122° 25.61'	103.93	0.12	980611.65	980676.20	-32.47	-43.97
45° 31.16'	122° 25.30'	108.20	0.13	980610.67	980676.20	-32.14	-44.10
45° 31.16'	122° 24.95'	113.38	0.13	980609.41	980676.20	-31.80	-44.34
45° 31.16'	122° 24.64'	109.72	0.14	980610.20	980676.20	-32.14	-44.26
45° 31.16'	122° 24.30'	103.93	0.15	980612.28	980676.20	-31.84	-43.31
45° 31.16'	122° 24.00'	99.66	0.15	980612.13	980676.20	-33.31	-44.30
45° 31.16'	122° 23.42'	76.19	0.17	980615.97	980676.20	-36.71	-45.07
45° 31.16'	122° 23.09'	66.44	0.17	980618.19	980676.20	-37.50	-44.76
45° 31.16'	122° 22.78'	67.66	0.18	980617.83	980676.20	-37.49	-44.87
45° 31.16'	122° 22.50'	68.88	0.18	980617.09	980676.20	-37.85	-45.37
45° 31.15'	122° 35.72'	128.88	0.32	980620.90	980676.18	-15.50	-29.59
45° 31.15'	122° 34.67'	79.85	0.04	980629.14	980676.18	-22.40	-31.29
45° 31.15'	122° 34.61'	79.85	0.04	980629.35	980676.18	-22.19	-31.08
45° 31.15'	122° 34.48'	80.16	0.04	980629.11	980676.18	-22.34	-31.26
45° 31.15'	122° 34.16'	82.29	0.03	980628.12	980676.18	-22.67	-31.83
45° 31.15'	122° 33.88'	84.73	0.03	980627.11	980676.18	-22.93	-32.37
45° 31.15'	122° 33.56'	84.73	0.03	980626.18	980676.18	-23.86	-33.30
45° 31.15'	122° 33.16'	85.34	0.03	980625.16	980676.18	-24.69	-34.20
45° 31.15'	122° 32.84'	85.95	0.03	980624.59	980676.18	-25.07	-34.65
45° 31.15'	122° 32.52'	88.39	0.03	980623.36	980676.18	-25.55	-35.40
45° 31.15'	122° 32.47'	88.23	0.03	980623.12	980676.18	-25.83	-35.67
45° 31.15'	122° 32.20'	89.30	0.03	980622.58	980676.18	-26.04	-36.00
45° 31.15'	122° 23.73'	97.53	0.16	980611.70	980676.18	-34.38	-45.13
45° 31.13'	122° 39.39'	13.99	0.14	980645.76	980676.16	-26.08	-27.51
45° 31.13'	122° 38.21'	48.16	0.07	980639.27	980676.16	-22.03	-27.35
45° 31.11'	122° 36.46'	63.89	0.10	980634.98	980676.13	-21.43	-28.48
45° 31.02'	122° 35.57'	124.65	1.73	980622.36	980675.99	-15.16	-27.36
45° 30.96'	122° 35.69'	151.76	2.05	980615.28	980675.90	-13.78	-28.70

TABLE II (Cont.)

Latitude	Longitude	Elev. meters	T. C. mgals	Observed Gravity mgals	Theoretical Gravity mgals	F. A. Anomaly mgals	C. B. Anomaly mgals
45° 30.95'	122° 34.81'	80.77	0.04	980629.91	980675.88	-21.05	-30.03
45° 30.89'	122° 32.47'	93.84	0.03	980621.98	980675.79	-24.85	-35.31
45° 30.85'	122° 36.05'	95.26	0.18	980629.27	980675.73	-17.07	-27.54
45° 30.83'	122° 34.36'	79.21	0.03	980629.30	980675.70	-21.96	-30.78
45° 30.82'	122° 35.28'	122.89	0.97	980622.10	980675.69	-15.66	-28.43
45° 30.81'	122° 34.07'	79.77	0.03	980628.65	980675.67	-22.40	-31.29
45° 30.79'	122° 35.51'	195.04	2.55	980605.51	980675.64	- 9.94	-29.19
45° 30.79'	122° 29.72'	73.36	0.05	980621.14	980675.64	-31.86	-40.01
45° 30.78'	122° 33.83'	79.87	0.03	980628.11	980675.63	-22.87	-31.77
45° 30.74'	122° 34.81'	78.89	0.04	980630.26	980675.57	-20.96	-29.74
45° 30.73'	122° 37.29'	48.28	0.05	980639.14	980675.55	-21.51	-26.86
45° 30.73'	122° 36.95'	50.48	0.07	980638.50	980675.55	-21.47	-27.05
45° 30.73'	122° 36.67'	55.33	0.09	980637.13	980675.55	-21.35	-27.44
45° 30.73'	122° 36.47'	61.01	0.11	980635.94	980675.55	-20.78	-27.50
45° 30.73'	122° 36.33'	72.55	0.12	980633.78	980675.55	-19.38	-27.37
45° 30.73'	122° 34.80'	78.88	0.04	980630.27	980675.55	-20.94	-29.71
45° 30.72'	122° 36.21'	80.50	0.15	980632.52	980675.54	-18.17	-27.03
45° 30.72'	122° 36.05'	88.17	0.18	980630.84	980675.54	-17.49	-27.16
45° 30.72'	122° 34.63'	80.18	0.04	980629.80	980675.54	-20.99	-29.92
45° 30.70'	122° 32.47'	92.11	0.02	980622.28	980675.50	-24.79	-35.07
45° 30.67'	122° 35.80'	126.79	0.63	980622.56	980675.46	-13.77	-27.32
45° 30.57'	122° 35.80'	90.31	0.30	980630.12	980675.31	-17.32	-27.12
45° 30.52'	122° 34.80'	79.33	0.04	980630.72	980675.24	-20.03	-28.86
45° 30.47'	122° 32.47'	92.50	0.02	980622.69	980675.17	-23.93	-34.25
45° 30.45'	122° 29.71'	71.97	0.06	980621.14	980675.14	-31.79	-39.78
45° 30.32'	122° 35.66'	65.84	0.15	980634.84	980674.94	-19.78	-26.99
45° 30.31'	122° 34.67'	80.77	0.04	980630.03	980674.92	-19.97	-28.95
45° 30.28'	122° 29.73'	74.97	0.06	980620.18	980674.87	-31.56	-39.88
45° 30.26'	122° 32.47'	91.65	0.03	980622.94	980674.84	-23.61	-33.83
45° 30.20'	122° 35.66'	67.68	0.11	980633.94	980674.76	-19.93	-27.38
45° 30.10'	122° 34.67'	71.62	0.04	980632.67	980674.60	-19.83	-27.80

TABLE II (Cont.)

Latitude	Longitude	Elev. meters	T. C. mgals	Observed Gravity mgals	Theoretical Gravity mgals	F. A. Anomaly mgals	C. B. Anomaly mgals
45° 30.07'	122° 29.74'	77.06	0.08	980619.00	980674.55	-31.77	-40.30
45° 30.03'	122° 32.62'	87.72	0.04	980624.43	980674.50	-23.00	-32.77
45° 29.96'	122° 31.06'	67.23	0.09	980624.79	980674.40	-28.86	-36.29
45° 29.95'	122° 30.74'	68.88	0.09	980623.57	980674.38	-29.55	-37.16
45° 29.91'	122° 35.48'	70.82	0.06	980632.90	980674.32	-19.56	-27.42
45° 29.90'	122° 29.72'	76.33	0.12	980618.89	980674.30	-31.85	-40.27
45° 29.89'	122° 34.64'	72.23	0.03	980632.50	980674.29	-19.50	-27.54
45° 29.88'	122° 25.48'	99.21	0.12	980607.79	980674.28	-35.87	-46.84
45° 29.88'	122° 25.19'	103.12	0.10	980606.45	980674.28	-36.00	-47.43
45° 29.87'	122° 31.43'	68.95	0.06	980625.29	980674.26	-27.69	-35.33
45° 29.87'	122° 25.79'	96.98	0.15	980608.81	980674.26	-35.52	-46.22
45° 29.87'	122° 24.77'	112.69	0.09	980604.16	980674.26	-35.32	-47.83
45° 29.84'	122° 27.24'	103.63	0.14	980608.11	980674.21	-34.12	-45.56
45° 29.84'	122° 26.77'	117.34	0.17	980605.25	980674.21	-32.74	-45.69
45° 29.83'	122° 26.50'	108.35	0.20	980606.83	980674.20	-33.93	-45.84
45° 29.83'	122° 26.27'	97.53	0.22	980609.05	980674.20	-35.05	-45.73
45° 29.83'	122° 26.02'	93.49	0.18	980609.68	980674.20	-35.66	-45.93
45° 29.82'	122° 30.27'	70.71	0.11	980622.09	980674.19	-30.27	-38.07
45° 29.82'	122° 27.05'	108.81	0.15	980607.06	980674.18	-33.54	-45.55
45° 29.80'	122° 30.21'	74.06	0.13	980620.17	980674.15	-31.12	-39.27
45° 29.78'	122° 29.04'	80.99	0.08	980615.64	980674.13	-33.50	-42.47
45° 29.78'	122° 27.42'	94.48	0.14	980610.33	980674.12	-34.63	-45.06
45° 29.75'	122° 35.64'	69.42	0.04	980633.11	980674.08	-19.55	-27.27
45° 29.71'	122° 32.62'	78.35	0.05	980626.88	980674.02	-22.96	-31.67
45° 29.71'	122° 26.00'	94.48	0.36	980608.71	980674.02	-36.15	-46.36
45° 29.70'	122° 27.57'	91.59	0.15	980610.73	980674.01	-35.01	-45.10
45° 29.69'	122° 29.74'	78.05	0.26	980617.88	980673.99	-32.03	-40.49
45° 29.68'	122° 29.63'	78.85	0.25	980617.42	980673.97	-32.22	-40.78
45° 29.66'	122° 24.51'	119.48	0.08	980602.43	980673.95	-34.65	-47.92
45° 29.65'	122° 34.64'	71.90	0.02	980632.33	980673.93	-19.41	-27.42
45° 29.62'	122° 29.33'	84.03	0.14	980615.38	980673.88	-32.57	-41.82

TABLE II (Cont.)

Latitude	Longitude	Elev. meters	T.C. mgals	Observed Gravity mgals	Theoretical Gravity mgals	F.A. Anomaly mgals	C.B. Anomaly mgals
45° 29.60'	122° 26.01'	112.77	0.56	980604.33	980673.85	-34.73	-46.77
45° 29.60'	122° 24.28'	124.20	0.08	980601.75	980673.85	-33.77	-47.57
45° 29.58'	122° 35.65'	68.80	0.02	980633.01	980673.82	-19.58	-27.25
45° 29.52'	122° 26.01'	129.54	0.90	980600.74	980673.73	-33.02	-46.60
45° 29.51'	122° 27.82'	85.64	0.19	980611.84	980673.71	-35.44	-44.82
45° 29.51'	122° 23.87'	128.16	0.08	980601.09	980673.72	-33.08	-47.32
45° 29.49'	122° 22.29'	124.96	0.24	980600.12	980673.69	-35.00	-48.73
45° 29.48'	122° 28.64'	87.32	0.12	980612.63	980673.66	-34.09	-43.73
45° 29.46'	122° 25.91'	154.83	1.04	980594.59	980673.64	-31.62	-47.53
45° 29.45'	122° 37.87'	40.44	0.10	980639.85	980673.62	-21.29	-25.72
45° 29.44'	122° 36.09'	69.72	0.03	980632.65	980673.60	-19.44	-27.21
45° 29.44'	122° 34.64'	72.78	0.02	980631.92	980673.61	-19.23	-27.35
45° 29.43'	122° 39.11'	29.42	0.27	980643.88	980673.60	-20.64	-23.65
45° 29.43'	122° 38.98'	22.54	0.21	980645.22	980673.60	-21.42	-23.73
45° 29.43'	122° 38.76'	16.55	0.18	980646.45	980673.60	-22.04	-23.71
45° 29.43'	122° 38.51'	16.35	0.14	980645.87	980673.60	-22.68	-24.37
45° 29.43'	122° 38.17'	25.01	0.12	980643.81	980673.60	-22.07	-24.74
45° 29.43'	122° 37.63'	43.77	0.10	980639.02	980673.60	-21.07	-25.86
45° 29.43'	122° 37.29'	46.26	0.11	980638.44	980673.60	-20.88	-25.94
45° 29.43'	122° 37.06'	64.98	0.11	980633.92	980673.60	-19.62	-26.78
45° 29.43'	122° 36.84'	73.51	0.08	980631.88	980673.60	-19.03	-27.17
45° 29.43'	122° 36.48'	69.76	0.04	980632.73	980673.60	-19.34	-27.10
45° 29.43'	122° 35.65'	69.20	0.02	980632.71	980673.60	-19.53	-27.24
45° 29.43'	122° 35.10'	69.11	0.02	980632.43	980673.60	-19.84	-27.54
45° 29.43'	122° 34.34'	83.61	0.02	980628.60	980673.60	-19.19	-28.52
45° 29.43'	122° 23.54'	134.41	0.09	980599.64	980673.59	-32.47	-47.41
45° 29.42'	122° 34.16'	82.59	0.02	980628.75	980673.59	-19.35	-28.56
45° 29.42'	122° 28.44'	88.62	0.13	980611.90	980673.58	-34.33	-44.11
45° 29.41'	122° 33.59'	78.16	0.03	980628.84	980673.58	-20.61	-29.32
45° 29.40'	122° 33.20'	74.11	0.04	980628.82	980673.56	-21.86	-30.11
45° 29.40'	122° 32.87'	71.82	0.05	980628.48	980673.55	-22.90	-30.88

TABLE II (Cont.)

Latitude	Longitude	Elev. meters	T.C. mgals	Observed Gravity mgals	Theoretical Gravity mgals	F.A. Anomaly mgals	C.B. Anomaly mgals
45° 29.40'	122° 32.68'	70.46	0.06	980628.26	980673.55	-23.54	-31.36
45° 29.40'	122° 32.21'	64.75	0.08	980628.06	980673.55	-25.50	-32.66
45° 29.40'	122° 31.87'	62.38	0.10	980627.33	980673.55	-26.97	-33.84
45° 29.40'	122° 31.44'	61.51	0.14	980626.12	980673.55	-28.44	-35.18
45° 29.31'	122° 27.99'	81.22	0.20	980612.77	980673.42	-35.59	-44.46
45° 29.30'	122° 26.17'	251.91	1.77	980572.67	980673.40	-22.98	-49.37
45° 29.29'	122° 22.29'	153.92	0.19	980592.92	980673.38	-32.96	-49.98
45° 29.27'	122° 25.95'	191.10	1.17	980586.64	980673.36	-27.75	-47.94
45° 29.25'	122° 26.26'	259.68	3.32	980570.65	980673.32	-22.53	-48.24
45° 29.21'	122° 34.65'	69.03	0.03	980632.80	980673.27	-19.16	-26.85
45° 29.21'	122° 23.54'	137.73	0.09	980598.35	980673.27	-32.42	-47.72
45° 29.17'	122° 26.22'	235.00	1.50	980577.46	980673.20	-23.23	-47.99
45° 29.08'	122° 22.29'	147.82	0.15	980593.71	980673.08	-33.74	-50.11
45° 29.06'	122° 26.21'	222.80	1.41	980579.93	980673.04	-24.36	-47.85
45° 29.01'	122° 34.65'	67.81	0.04	980632.56	980672.97	-19.48	-27.02
45° 29.00'	122° 23.52'	126.49	0.09	980599.84	980672.95	-34.07	-48.11
45° 28.86'	122° 22.29'	143.25	0.13	980594.23	980672.74	-34.30	-50.18
45° 28.78'	122° 34.61'	69.49	0.05	980632.27	980672.62	-18.90	-26.62
45° 28.74'	122° 23.52'	133.80	0.10	980597.61	980672.56	-33.66	-48.52
45° 28.64'	122° 30.71'	75.52	0.72	980619.07	980672.41	-30.03	-37.76
45° 28.62'	122° 22.29'	149.35	0.13	980591.60	980672.38	-34.69	-51.26
45° 28.61'	122° 23.52'	138.98	0.10	980595.92	980672.36	-33.55	-48.99
45° 28.60'	122° 32.15'	84.12	0.29	980623.23	980672.34	-23.15	-32.26
45° 28.58'	122° 32.80'	64.49	0.23	980629.53	980672.31	-22.88	-29.85
45° 28.56'	122° 34.61'	71.62	0.07	980631.77	980672.29	-18.41	-26.35
45° 28.46'	122° 23.52'	143.86	0.11	980594.67	980672.14	-33.08	-49.05
45° 28.45'	122° 29.59'	96.99	0.21	980610.49	980672.12	-31.70	-42.33
45° 28.44'	122° 32.83'	65.32	0.34	980629.62	980672.11	-22.33	-29.30
45° 28.41'	122° 22.29'	162.45	0.12	980588.20	980672.06	-33.73	-51.77
45° 28.37'	122° 25.83'	225.85	0.59	980577.48	980672.01	-24.83	-49.48
45° 28.35'	122° 34.61'	68.58	0.09	980632.26	980671.97	-18.55	-26.13

TABLE II (Cont.)

Latitude	Longitude	Elev. meters	T.C. mgals	Observed Gravity mgals	Theoretical Gravity mgals	F.A. Anomaly mgals	C.B. Anomaly mgals
45° 28.25'	122° 32.82'	111.30	0.54	980620.62	980671.82	-16.85	-28.75
45° 28.25'	122° 23.48'	132.13	0.12	980596.74	980671.82	-34.30	-48.95
45° 28.20'	122° 25.99'	234.69	0.62	980575.49	980671.74	-23.82	-49.44
45° 28.18'	122° 22.29'	146.30	0.12	980590.38	980671.72	-36.18	-52.41
45° 28.13'	122° 34.59'	65.53	0.11	980632.97	980671.64	-18.45	-25.67
45° 28.11'	122° 32.82'	128.74	0.64	980617.95	980671.61	-13.93	-27.68
45° 28.06'	122° 29.12'	101.94	0.15	980607.84	980671.54	-32.24	-43.48
45° 28.01'	122° 23.84'	119.78	0.30	980599.01	980671.46	-35.48	-48.57
45° 27.98'	122° 32.43'	181.38	0.63	980605.66	980671.41	-9.78	-29.43
45° 27.97'	122° 22.29'	150.87	0.12	980588.73	980671.42	-36.13	-52.87
45° 27.97'	122° 32.83'	159.23	0.73	980611.80	980671.40	-10.46	-27.53
45° 27.91'	122° 32.64'	153.93	0.68	980612.67	980671.40	-11.23	-27.76
45° 27.91'	122° 34.66'	59.43	0.13	980634.12	980671.31	-18.85	-25.36
45° 27.90'	122° 28.80'	104.69	0.17	980605.87	980671.30	-33.12	-44.66
45° 27.89'	122° 26.18'	253.28	0.67	980572.28	980671.29	-20.84	-48.48
45° 27.88'	122° 33.26'	116.85	0.61	980621.74	980671.27	-13.47	-25.91
45° 27.88'	122° 33.10'	132.94	0.65	980618.00	980671.27	-12.24	-26.45
45° 27.88'	122° 32.92'	152.75	0.76	980613.39	980671.27	-10.74	-27.05
45° 27.79'	122° 36.54'	50.48	0.14	980635.68	980671.13	-19.87	-25.37
45° 27.76'	122° 36.92'	30.26	0.15	980640.44	980671.08	-21.30	-24.53
45° 27.76'	122° 31.59'	175.56	0.44	980603.34	980671.08	-13.56	-32.74
45° 27.75'	122° 26.21'	251.15	0.62	980573.09	980671.07	-20.47	-47.93
45° 27.74'	122° 36.07'	76.39	0.14	980629.47	980671.06	-18.01	-26.42
45° 27.72'	122° 22.29'	135.94	0.19	980590.06	980671.02	-39.01	-54.02
45° 27.71'	122° 34.64'	60.92	0.18	980633.85	980671.01	-18.36	-24.99
45° 27.69'	122° 35.66'	74.32	0.09	980630.34	980670.99	-17.71	-25.93
45° 27.69'	122° 23.82'	127.10	0.47	980596.77	980670.98	-34.99	-48.72
45° 27.68'	122° 34.95'	57.85	0.14	980634.01	980670.96	-19.10	-25.43
45° 27.68'	122° 30.14'	158.46	0.37	980601.60	980670.96	-20.46	-37.80
45° 27.67'	122° 34.69'	60.96	0.15	980634.52	980670.95	-17.62	-24.29
45° 27.66'	122° 34.02'	83.85	0.50	980628.77	980670.93	-16.28	-25.16

TABLE II (Cont.)

Latitude	Longitude	Elev. meters	T. C. mgals	Observed Gravity mgals	Theoretical Gravity mgals	F. A. Anomaly mgals	C. B. Anomaly mgals
45° 27.53'	122° 22.29'	146.91	0.21	980586.62	980670.74	-38.78	-54.99
45° 27.43'	122° 34.66'	63.09	0.17	980633.61	980670.59	-17.51	-24.40
45° 27.37'	122° 28.55'	112.63	0.21	980602.77	980670.49	-32.97	-45.35
45° 27.29'	122° 33.01'	333.17	4.37	980569.52	980670.38	+1.96	-30.91
45° 27.27'	122° 31.27'	160.30	0.40	980605.29	980670.35	-15.58	-33.10
45° 27.27'	122° 30.80'	153.58	0.33	980604.58	980670.35	-18.38	-35.22
45° 27.27'	122° 22.29'	179.83	0.19	980579.09	980670.35	-35.76	-55.67
45° 27.26'	122° 31.56'	183.00	0.44	980602.21	980670.33	-11.65	-31.67
45° 27.25'	122° 33.11'	325.28	4.12	980571.21	980670.32	+1.28	-30.96
45° 27.22'	122° 32.27'	254.79	1.20	980589.27	980670.28	-2.38	-29.66
45° 27.20'	122° 34.66'	64.00	0.18	980633.47	980670.24	-17.02	-23.99
45° 27.18'	122° 32.80'	318.46	3.94	980573.56	980670.21	+1.62	-30.03
45° 27.13'	122° 27.94'	139.83	0.57	980596.44	980670.14	-30.54	-45.60
45° 27.10'	122° 22.29'	179.83	0.17	980577.34	980670.10	-37.27	-57.20
45° 27.08'	122° 32.15'	217.83	0.95	980596.75	980670.06	-6.09	-29.49
45° 27.05'	122° 32.50'	295.29	2.27	980580.13	980670.01	+1.25	-29.49
45° 27.03'	122° 33.72'	166.00	0.92	980610.47	980669.99	-8.30	-25.94
45° 26.95'	122° 34.66'	61.87	0.20	980633.31	980669.87	-17.46	-24.18
45° 26.91'	122° 34.66'	61.78	0.20	980632.79	980669.81	-17.94	-24.66
45° 26.90'	122° 35.97'	51.94	0.07	980634.40	980669.79	-19.35	-25.09
45° 26.90'	122° 35.88'	50.55	0.07	980634.81	980669.79	-19.38	-24.96
45° 26.89'	122° 35.64'	49.31	0.11	980635.09	980669.78	-19.46	-24.87
45° 26.86'	122° 22.29'	156.97	0.26	980579.88	980669.73	-41.41	-58.69
45° 26.85'	122° 35.39'	58.42	0.13	980633.08	980669.72	-18.61	-25.01
45° 26.84'	122° 35.35'	65.13	0.14	980631.68	980669.70	-17.92	-25.06
45° 26.84'	122° 35.15'	64.75	0.15	980631.79	980669.70	-17.92	-25.02
45° 26.84'	122° 34.98'	65.29	0.16	980631.75	980669.70	-17.79	-24.93
45° 26.84'	122° 31.58'	140.54	0.40	980610.45	980669.70	-15.88	-31.19
45° 26.84'	122° 28.43'	108.11	0.26	980602.94	980669.70	-33.40	-45.22
45° 26.82'	122° 32.56'	271.72	1.74	980586.28	980669.68	+0.45	-28.18
45° 26.82'	122° 31.77'	151.90	0.42	980608.80	980669.68	-14.00	-30.56

TABLE II (Cont.)

Latitude	Longitude	Elev. meters	T. C. mgals	Observed Gravity mgals	Theoretical Gravity mgals	F. A. Anomaly mgals	C. B. Anomaly mgals
45° 26.82'	122° 30.81'	166.33	0.60	980602.00	980669.68	-16.35	-34.34
45° 26.77'	122° 33.99'	105.71	0.54	980623.86	980669.59	-13.10	-24.38
45° 26.76'	122° 34.31'	68.09	0.33	980631.76	980669.58	-16.81	-24.09
45° 26.70'	122° 34.66'	55.47	0.19	980635.14	980669.49	-17.23	-23.24
45° 26.64'	122° 22.90'	166.58	0.43	980581.35	980669.39	-36.63	-54.82
45° 26.64'	122° 22.29'	173.12	0.23	980576.09	980669.40	-39.88	-59.01
45° 26.62'	122° 33.87'	101.17	0.54	980625.29	980669.37	-12.85	-23.63
45° 26.61'	122° 33.73'	117.34	0.65	980621.75	980669.36	-11.40	-23.87
45° 26.54'	122° 31.84'	132.13	0.40	980612.96	980669.25	-15.52	-29.89
45° 26.46'	122° 34.66'	54.86	0.18	980635.51	980669.13	-16.69	-22.64
45° 26.43'	122° 22.29'	167.03	0.11	980576.58	980669.09	-40.96	-59.52
45° 26.39'	122° 32.78'	165.43	0.89	980608.90	980669.03	-9.07	-26.67
45° 26.39'	122° 25.99'	173.77	0.15	980587.02	980669.03	-28.38	-47.66
45° 26.33'	122° 33.78'	93.89	0.46	980626.92	980668.94	-13.04	-23.08
45° 26.24'	122° 22.29'	171.29	0.12	980583.01	980668.80	-32.93	-51.96
45° 26.23'	122° 34.66'	52.42	0.18	980636.04	980668.78	-16.57	-22.25
45° 26.20'	122° 33.75'	90.90	0.34	980627.55	980668.74	-13.14	-22.96
45° 26.13'	122° 28.28'	111.26	0.39	980603.02	980668.63	-31.27	-43.31
45° 26.04'	122° 34.67'	47.24	0.17	980637.01	980668.50	-16.91	-22.02
45° 26.02'	122° 33.06'	97.03	0.40	980624.08	980668.46	-14.44	-24.89
45° 26.02'	122° 22.29'	157.27	0.15	980577.77	980668.46	-42.15	-59.58
45° 25.98'	122° 34.28'	49.73	0.21	980636.03	980668.40	-17.02	-22.37
45° 25.98'	122° 34.03'	61.33	0.24	980633.62	980668.41	-15.87	-22.48
45° 25.98'	122° 32.78'	101.37	0.45	980622.41	980668.41	-14.72	-25.61
45° 25.97'	122° 34.70'	46.58	0.17	980636.03	980668.39	-17.99	-23.03
45° 25.89'	122° 32.53'	78.63	0.53	980622.97	980668.28	-21.04	-29.30
45° 25.87'	122° 31.59'	132.26	0.55	980610.19	980668.24	-17.23	-31.46
45° 25.84'	122° 22.93'	168.85	0.45	980579.12	980668.19	-36.96	-55.39
45° 25.81'	122° 34.67'	39.62	0.17	980638.33	980668.15	-17.59	-21.86
45° 25.80'	122° 32.22'	117.34	0.34	980615.33	980668.14	-16.60	-29.37
45° 25.79'	122° 22.50'	150.38	0.17	980579.77	980668.11	-41.94	-58.57

TABLE II (Cont.)

Latitude	Longitude	Elev. meters	T.C. mgals	Observed Gravity mgals	Theoretical Gravity mgals	F.A. Anomaly mgals	C.B. Anomaly mgals
45° 25.79'	122° 22.42'	150.57	0.17	980580.63	980668.12	-41.03	-57.69
45° 25.72'	122° 32.22'	106.71	0.32	980617.57	980668.02	-17.51	-29.12
45° 25.59'	122° 31.65'	114.94	0.21	980613.77	980667.82	-18.58	-31.22
45° 25.58'	122° 27.74'	189.87	0.34	980584.51	980667.81	-24.70	-45.58
45° 25.56'	122° 34.55'	28.95	0.16	980641.62	980667.78	-17.22	-20.30
45° 25.40'	122° 22.58'	159.10	0.17	980578.96	980667.53	-39.47	-57.08
45° 25.33'	122° 23.84'	179.62	0.24	980579.54	980667.43	-32.46	-52.30
45° 25.32'	122° 34.36'	40.23	0.15	980638.96	980667.41	-16.04	-20.39
45° 25.13'	122° 34.22'	45.71	0.14	980637.17	980667.13	-15.85	-20.82
45° 25.09'	122° 24.74'	178.86	0.12	980581.87	980667.07	-30.00	-49.88
45° 25.08'	122° 25.36'	188.06	0.14	980581.03	980667.05	-27.99	-48.87
45° 25.05'	122° 27.32'	160.08	0.17	980589.17	980667.01	-28.44	-46.16
45° 24.90'	122° 34.06'	45.71	0.13	980635.38	980666.78	-17.29	-22.27
45° 24.90'	122° 27.71'	160.62	0.18	980591.59	980666.78	-25.62	-43.40
45° 24.88'	122° 36.00'	49.59	0.29	980640.32	980666.75	-11.13	-16.39
45° 24.88'	122° 22.90'	184.40	0.13	980574.98	980666.74	-34.86	-55.34
45° 24.84'	122° 28.05'	157.27	0.18	980592.70	980666.70	-25.46	-42.86
45° 24.72'	122° 29.06'	123.74	0.19	980603.72	980666.52	-24.61	-38.25
45° 24.70'	122° 34.00'	45.71	0.12	980634.77	980666.48	-17.60	-22.59
45° 24.69'	122° 36.28'	95.83	0.31	980632.37	980666.47	-4.53	-14.93
45° 24.66'	122° 35.35'	37.44	0.15	980638.47	980666.42	-16.40	-20.44
45° 24.64'	122° 29.62'	99.66	0.21	980607.23	980666.39	-28.40	-39.33
45° 24.63'	122° 28.63'	143.25	0.18	980597.93	980666.38	-24.24	-40.07
45° 24.62'	122° 31.39'	44.80	0.30	980626.33	980666.37	-26.21	-30.92
45° 24.60'	122° 30.98'	46.02	0.33	980623.92	980666.34	-28.22	-33.03
45° 24.60'	122° 30.34'	51.20	0.39	980619.77	980666.34	-30.77	-36.10
45° 24.55'	122° 31.76'	41.45	0.27	980628.03	980666.26	-25.44	-29.80
45° 24.48'	122° 32.19'	39.26	0.25	980630.07	980666.15	-23.97	-28.10
45° 24.47'	122° 33.87'	42.23	0.13	980633.88	980666.13	-19.21	-23.81
45° 24.47'	122° 33.64'	33.45	0.15	980635.50	980666.13	-20.30	-23.89
45° 24.47'	122° 33.21'	35.11	0.18	980634.33	980666.13	-20.96	-24.71